

# Black Holes merging with Low Mass Gap Objects inside Globular Clusters

Konstantinos Kritos<sup>1,\*</sup> and Ilias Cholis<sup>2,†</sup>

<sup>1</sup>*Physics Division, National Technical University of Athens, Zografou, Athens, 15780, Greece*

<sup>2</sup>*Department of Physics, Oakland University, Rochester, Michigan, 48309, USA*

(Dated: January 6, 2022)

Recently, the LIGO-Virgo collaborations have reported the coalescence of a binary involving a black hole and a low-mass gap object (LMGO) with mass in the range  $\sim 2.5\text{--}5M_{\odot}$ . Such detections, challenge our understanding of the black hole and neutron star mass spectrum, as well as how such binaries evolve especially if isolated. In this work we study the dynamical formation of compact object pairs, via multiple binary-single exchanges that occur at the cores of globular clusters. We start with a population of binary star systems, which interact with single compact objects as first generation black holes and LMGOs. We evaluate the rate of exchange interactions leading to the formation of compact object binaries. Our calculations include all possible types of binary-single exchange interactions and also the interactions of individual stars with compact object binaries that can evolve their orbital properties, leading to their eventual merger. We perform our calculations for the full range of the observed Milky Way globular cluster environments. We find that the exchanges are efficient in forming hard compact object binaries at the cores of dense astrophysical stellar environments. Furthermore, if the population size of the LMGOs is related to that of neutron stars, the inferred merger rate density of black hole-LMGO binaries inside globular clusters in the local Universe is estimated to be about  $0.1\text{ Gpc}^{-3}\text{yr}^{-1}$ .

## I. INTRODUCTION

Globular clusters are complex environments where single and binary stars, neutron stars (NSs) and black holes (BHs), coexist and can have strong dynamical interactions. Those interactions can lead to the creation of compact object-star or compact object-compact object binaries. In the Milky Way we have observed so far more than 160 such systems for many of which we have well-measured total mass and density profiles [1, 2]. Moreover, in some of these environments the compact objects will have multiple interactions as has been shown in [3–10]. Thus, we expect different combinations of binaries between the stars and the compact objects and the compact objects themselves, which may even lead to runaway mergers [11–19].

One exciting possibility is that among the many compact objects inhabiting globular clusters, are low mass gap objects (LMGOs). These are objects with mass larger than the expected NS upper mass limit of approximately  $2.5 M_{\odot}$  (see [20] for a relevant review), and lower than the empirical lower stellar-mass BHs from core collapses of  $5 M_{\odot}$  [21–23] (see however [24]). In fact, recently the Virgo and the LIGO Scientific collaborations reported the detection of a merger event (GW190814) between a  $23.2^{+1.1}_{-1.0} M_{\odot}$  BH and a  $2.59^{+0.08}_{-0.09} M_{\odot}$  LMGO [25]. This discovery is even more intriguing due to its unusual high mass ratio. Its possible explanations include the discovery of the least massive BH [26, 27], the most massive NS [28–35] ever observed, an exotic compact object

[36–39] or a primordial black hole [40–42]. Additionally, such BH-LMGO pairs may be formed inside dense clusters through complex triple and hierarchical quadruple systems [43–47], or as isolated pairs [48], or be the result of mass accretion of a NS from the supernova envelope of its progenitor in an isolated compact binary [49]. Finally, the peculiar derived compact objects mass-values may just be due to GW190814 being a lensed merger event [50].

Over the past few years the LIGO-Virgo collaboration have detected double neutron star mergers [51, 52], with the merged product being in the mass gap interval. A fraction of objects in the mass range of LMGOs certainly originated from the coalescence of two neutron stars with the product having a mass around  $3M_{\odot}$ . While this may not be the only mechanism to create LMGOs (see for instance [53]), in this work we are not concerned with the nature of the LMGOs. Instead, we take their number solely coming from double neutron star mergers. This is a conservative choice which also uses the fact that the  $2.59M_{\odot}$  object lies in the mass range of double neutron star mergers [6].

We implement a simple model to evaluate the merger rate of BH-LMGO mergers formed in Milky Way globular cluster-type environments. We start with star-star binaries and through successive binary-single exchanges end in creating BH-BH, BH-LMGO and LMGO-LMGO binaries. We monitor the different populations of single compact objects i.e. BHs and LMGOs, as well as the different combinations of star/LMGO/BH binary populations. We rely on a qualitative description of the mass function for the populations we consider, and take monochromatic mass spectra for the stars, the LMGOs and the BHs; but also include the presence of second gen-

\* ge16004@central.ntua.gr

† cholis@oakland.edu, ORCID: orcid.org/0000-0002-3805-6478

eration black holes with mass nearly double that of the first generation ones. We demonstrate that BH-LMGO pairs can be produced and coalesce in a dynamical environment, where successive exchange events and hardening interactions with third less massive objects take place.

This paper is organized as follows. In section II we describe the setup to calculate the formation of compact binaries via exchanges inside stellar clusters and also how their orbital properties evolve. Then, in section III we present and discuss our findings on the time evolution of binary populations and their merger rates. Our work provides a realistic estimate of the minimum contribution globular cluster environments have on the BH-LMGO merger rates. Finally, we give our conclusions in section IV.

## II. METHODOLOGY AND ASSUMPTIONS

We assume that initially all LMGOs and all first generation black holes which we denote from here as “BH” start as single objects in the history of a given cluster. Only stars initially are in binaries. In this work compact object binaries are assembled through multiple exchanges from the smaller mass star-star pairs. We focus on the dynamical interactions between binaries and individual objects and take an agnostic approach on the origin of LMGOs, just assuming their number is set by the NS that remain in the clusters after the natal kicks. Binary stars can undergo exchange events with individual LMGOs or BHs leading to the creation of LMGO-star or BH-star binaries respectively. In Fig. 1 we depict those exchange interactions as channels “A” and “B”. Those binaries can then undergo further exchanges through channels “C”, “D”, “E” and “F” and create LMGO-LMGO, BH-LMGO or BH-BH binaries. In fact when the individual BHs come at close proximity to either the LMGO-LMGO or the BH-LMGO binaries further exchanges may take place leading to channels “G” and “H”.

All exchange channels are depicted in Fig. 1 by thin arrows and are identified by a letter. There is a flow of energy transferred from the pairs involving smaller mass objects into binaries involving BHs and LMGOs which then consequently merge via 3rd-body hardening evolution. The merger events are depicted as thick arrows and can lead to black holes. Those black holes can then be kicked out of the cluster due to a gravitational wave kick or remain in it and enter the population of compact objects available to dynamically interact. Due to what we will show to be a small number of LMGO-LMGO pairs and BH-LMGO pairs we ignore those objects. However, the BH-BH binaries merge into second generation black holes with mass approximately double the original first generation one. Those second generation black holes we denote as “BH’”. The BH’ objects that will remain in the clusters will then participate in exchange interactions with all type of existing binaries in the cluster cre-

ating also BH’-star, BH’-LMGO and BH’-BH binaries, through the exchange channels “I”, through “Q”. Those types of binaries are also connected through exchange interactions (channels “S”, “R” and “T”). Finally, “BH’-BH’” binaries can be created through exchange interactions of channels “U”, “V” and “W”.

In the following we describe all specific assumptions on the creation and evolution of these binaries.

### A. Hard binaries

A binary 1–2 with mass components  $m_1$  and  $m_2$  is defined as hard, when its semimajor axis (SMA) is smaller than  $a_H$ . We will refer to  $a_H$  as hardness SMA. This also defines the semimajor axis value below which a pair hardens at a constant rate via 3rd-body encounters with single stars of mass  $m_*$ . Assuming that  $m_1 \geq m_2 \gg m_*$ , this hardness SMA is given by [3, 54],

$$a_H \equiv \frac{Gm_2}{4\sigma_*^2} \approx 22.3 \times \left( \frac{m_2}{10M_\odot} \right) \left( \frac{\sigma_*}{10\text{km/s}} \right)^{-2} \text{AU}. \quad (1)$$

$\sigma_*$ , is the velocity dispersion of stars (see Appendix A for further details).

After a single 3rd-body encounter the orbital SMA and eccentricity change on average to,

$$a' = a \left[ 1 + \frac{H}{2\pi} \frac{m_*}{m_1+m_2} \right]^{-1}, \quad (2)$$

$$e' = e + K \left[ 1 + \frac{2\pi}{H} \frac{m_1+m_2}{m_*} \right]^{-1}, \quad (3)$$

where  $H$  and  $K$  are two parameters determined numerically. Past surveys [3, 54] have showed that  $H$  lies in the interval [15,20] and  $K$  is in [0,0.2]. We will use as reference the values of  $H = 20$  and  $K = 0.05$  for these parameters and will describe the impact of alternative choices which we find change only marginally our results.

Tight binaries harden until their SMA passes a critical value which we denote by  $a_{\text{GW}}$ . That SMA corresponds to the point where GW emission starts to dominate over the 3rd-body hardening process. Given that  $\rho_*$  is the mass density of stars and  $\sigma_{*,1-2}$  is the rms velocity of stars relative to the 1–2 pair (see Appendix A), then this critical SMA is approximately equal to, [4, 54],

$$\begin{aligned} a_{\text{GW}} &\simeq 0.05\text{AU} \times \left( \frac{\sigma_{*,1-2}}{10\text{km/s}} \right)^{1/5} \left( \frac{\rho_*}{10^5 M_\odot/\text{pc}^3} \right)^{-1/5} \\ &\times \left( \frac{H}{20} \right)^{-1/5} \left( \frac{m_1}{10M_\odot} \right)^{1/5} \left( \frac{m_2}{10M_\odot} \right)^{1/5} \\ &\times \left( \frac{m_1+m_2}{20M_\odot} \right)^{1/5} (1 - e_{\text{GW}}^2)^{-7/10} \\ &\times \left( 1 + \frac{73}{24} e_{\text{GW}}^2 + \frac{37}{96} e_{\text{GW}}^4 \right)^{1/5}, \end{aligned} \quad (4)$$

where  $e_{\text{GW}}$  is the eccentricity of the pair at the point when GW emission starts to dominate. After the binary

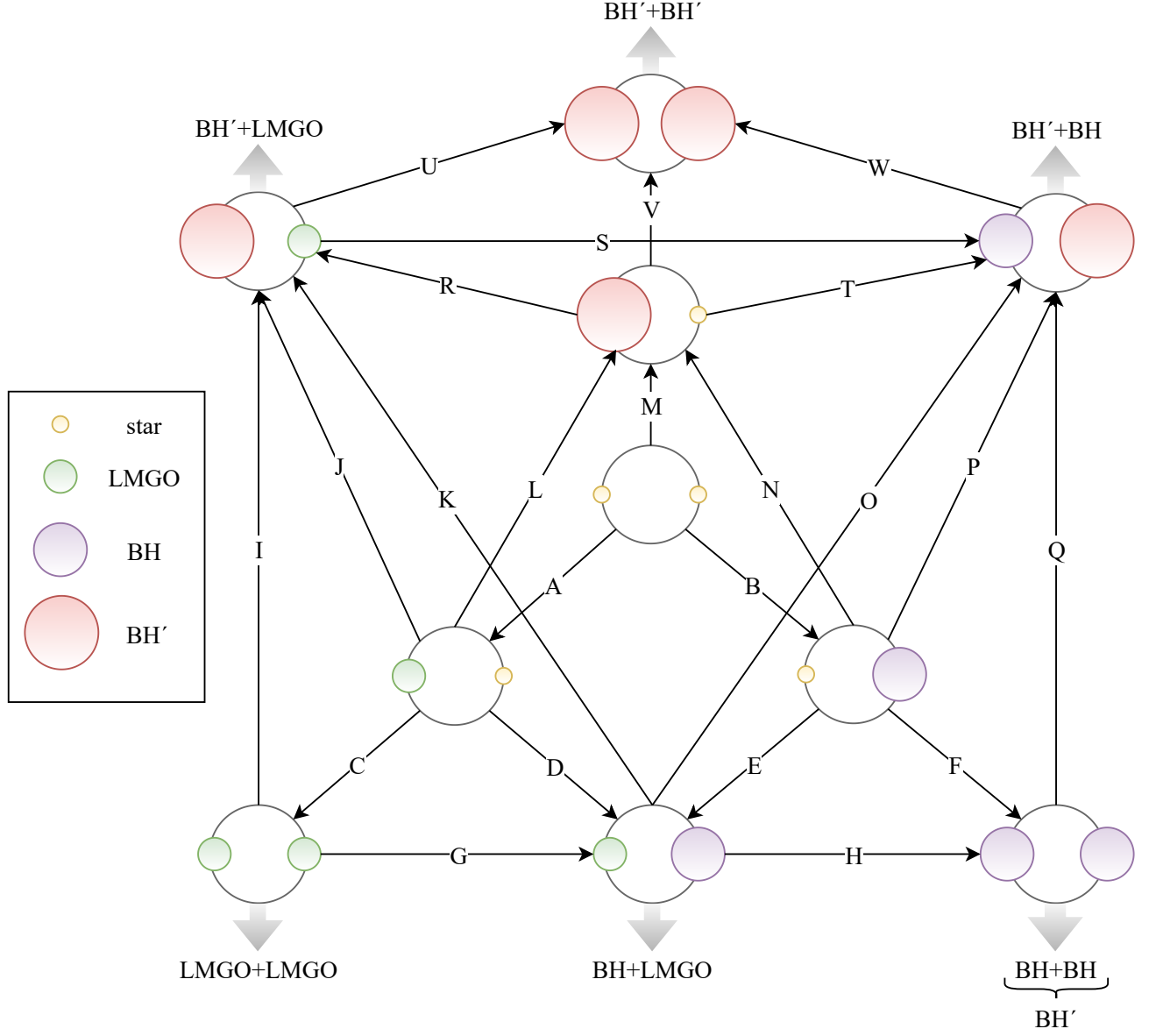


FIG. 1. A representation of the processes that we take into account for the formation of compact binaries inside globular clusters. Each narrow arrow implies a binary-single exchange and the corresponding rate contributes to the right hand side of the differential system in Eq. 9. Thick arrows represent the merger of binaries into more massive compact objects. In this work we take as reference values  $m_{\text{star}} = 1M_{\odot}$ ,  $m_{\text{LMGO}} = 3M_{\odot}$ ,  $m_{\text{BH}} = 10M_{\odot}$  and  $m_{\text{BH}'} = 19M_{\odot}$ .

enters this GW domination phase, the timescale required for it to merge solely due to the emission of GWs is given by [55],

$$T_{\text{GW}} \approx 1.5 \times 10^{11} \text{yr} \left( \frac{m_1}{10M_{\odot}} \right)^{-1} \left( \frac{m_2}{3M_{\odot}} \right)^{-1} \times \left( \frac{m_1 + m_2}{13M_{\odot}} \right)^{-1} \left( \frac{a_{\text{GW}}}{0.1\text{AU}} \right)^4 (1 - e_{\text{GW}}^2)^{7/2}. \quad (5)$$

In particular, if for instance  $e_{\text{GW}} = 0.9$ , then the above timescale is about 440Myr. For a numerical description of the 3rd-body and gravitational wave emission inside realistic globular cluster environments one can see [9, 10].

In this work for all binaries made out of two compact objects (i.e. LMGO-LMGO, BH-LMGO, BH'-LMGO, BH-BH, BH'-BH and BH'-BH') we include the effect of 3rd-body hardening interactions and evolve their SMA until they reach their respective value of  $a_{\text{GW}}$ ; calculated by Eq. 4 for the given binary masses  $m_1$ ,  $m_2$  and globular cluster environment  $(\sigma_*, \rho_*)$ . Once the binaries reach their respective  $a_{\text{GW}}$ , they will merge within  $T_{\text{GW}}$  calculated from Eq. 5.

## B. Number of compact objects in stellar clusters

Ref. [56] has showed that once a system of stellar mass black holes is created in the core of a globular cluster it remains for about 10 times the initial dynamical relaxation time. That relaxation time for the larger clusters relevant in this work, is more than a Gyr. Also, Refs. [57, 58] have shown that large numbers of black holes are retained inside globular clusters for a wide range of their properties. Recently Ref. [59] analyzed observational data from NGC 6397 supporting the presence of a core of compact objects at the center of that globular cluster. We choose for simplicity to take the volume that the stellar-mass black holes occupy  $V_{\text{BH}}$ , to be constant with time, and evolve our systems up to the Hubble time.

The number of first generation BHs in a given cluster is estimated from the initial stellar mass function and the natal kicks of the BHs. We take that only stars with mass larger than  $25M_{\odot}$  have collapsed into a BH. Based on the Kroupa stellar mass function [60],  $\approx 10\%$  of a cluster's mass  $M_{\text{cl}}$  has been in these stars. We assume that approximately  $1/3$  of the progenitor's mass collapses to the BH remnant [61]. Thus the total mass in first generation BHs that have been produced in the history of the cluster is about  $3\%$  of the cluster's mass,  $f_{\text{BH}} \approx 3\%$ . Of them only a fraction  $f_{\text{ret}}$  has been retained by the gravitational potential well of the cluster while the rest escaped due to their natal kick. For each cluster we evaluate  $f_{\text{ret}}$ ; on average we find it to be  $10\%$ . As we take all first generation BHs to be of mass  $m_{\text{BH}}$ , the number of retained BHs in a cluster is,

$$N_{\text{BH}} = f_{\text{ret}} f_{\text{BH}} \frac{M_{\text{cl}}}{m_{\text{BH}}} \quad (6)$$

$$\approx 30 \times \left( \frac{f_{\text{ret}}}{10\%} \right) \left( \frac{f_{\text{BH}}}{3\%} \right) \left( \frac{M_{\text{cl}}}{10^5 M_{\odot}} \right) \left( \frac{m_{\text{BH}}}{10 M_{\odot}} \right)^{-1}.$$

In a similar manner, we calculate the number of NSs, where for their retention fraction we have found it to be typically  $f_{\text{ret}}^{\text{NS}} \simeq 2\%$ , relying on [62] for their observed natal kicks distribution. As for every cluster the  $f_{\text{ret}}$  depends on the specific escape velocity, the more massive clusters retain a larger fraction of a larger number of such objects created in the first place. The fraction of the cluster's mass corresponding to NSs is also  $f_{\text{NS}} \approx 3\%$ , assuming that on average  $1/3$  of the progenitor's mass collapses to a NS.

Regarding the number of produced LMGOs, we assume that they originate from NS-NS mergers and that all NSs that didn't escape the cluster merged into LMGOs. Thus the number of LMGOs is simply half the number of the retained NSs, i.e.  $N_{\text{NSNS} \rightarrow \text{LMGO}} = \frac{N_{\text{NS}}}{2}$ . We also assume that those mergers happen very fast in the history of the cluster and essentially provide an initial population of LMGOs. However, we also study the case where the NS-NS binaries did not merge early in the history of the clusters, but instead evolve as a separate population of binaries. In that case those pairs progressively give LMGOs which once produced are added to

the population of single LMGOs and then are allowed to form binaries following the scheme of Fig. 1. The LMGOs from NS-NS mergers provide a candidate for these objects. The actual population size of LMGOs could be even larger if more exotic species of LMGOs are present as e.g. [19, 36, 63–65]. In Appendix B we provide results for different options setting the population size of LMGOs inside the cluster.

## C. Description of the model and initial conditions

The population of BH-LMGO pairs can be assembled through the exchanges designated by the arrow sequences A+D or B+E or A+C+G in Fig. 1. All pairs we consider are hard and do not get disrupted by stars [66]. We take that all binaries when first assembled have the largest possible SMA and evolve it with time. For the exchange events the new binary starts with a SMA that has the same value as that of the progenitor binary. This are conservative choices as they lead to the smaller number of coalescence events.

Regarding the SMA of the binaries, we consider a discretization of the SMA interval into bins and evolve each population in time. As a hard binary interacts with the surrounding stars, its SMA value becomes smaller by a factor of  $a'/a$  evaluated from Eq. 2<sup>1</sup>. That “jump” is performed following a rate of interaction between the binary and any close-by star. The velocity averaged interaction rate density at which a population of hard binaries  $1-2$  with mass components  $m_1$  and  $m_2$  and number density  $n_{1-2}$  interact with single objects  $3$  with mass  $m_3$  and number density  $n_3$  is given by [67],

$$\gamma_{\text{int}} = n_{1-2} n_3 \frac{2\sqrt{6\pi} G (m_1 + m_2 + m_3)}{\sigma_{3,1-2}} a. \quad (7)$$

Here,  $a$  is the SMA of the  $1-2$  system,  $G$  is the universal gravitational constant and  $\sigma_{3,1-2} = \sqrt{\langle v_{3,1-2}^2 \rangle}$  is the three dimensional velocity dispersion between the binary and the single object at infinity (see Appendix A). We note that, Eq. 7 is to be considered only at the gravitational focusing domination regime, i.e. holds valid only for strong interactions of stars with hard binaries. The total interaction rate  $\Gamma_{\text{int}}$  between a binary system  $1-2$  with a 3rd body is just,

$$\Gamma_{\text{int}} = \int_0^{V_{\text{BH}}} \gamma_{\text{int}} dV. \quad (8)$$

<sup>1</sup> We take a logarithmically spaced binning with 100 slots in total. Every binary, for example a BH-LMGO will harden due 3rd-body interactions. For instance after its  $i$ -th such interaction  $a_{\text{BH-LMGO}}(i) = a_{\text{BH-LMGO}}(i-1) \cdot f_{\text{H,BH-LMGO}}$ ; where  $a_{\text{BH-LMGO}}(1) = a_{\text{H,BH-LMGO}}$  from Eq. 1 and  $f_{\text{H,BH-LMGO}}$  is evaluated from Eq. 2 for  $m_* = 1M_{\odot}$ ,  $m_1 = 10M_{\odot}$ ,  $m_2 = 3M_{\odot}$ . As  $a_{\text{BH-LMGO}}$  is reduced the BH-LMGO binary will “jump” between these slots.

The set of differential equation describing the evolution

of the number of single compact objects and their binaries is,

$$\dot{N}_{\text{LMGO}} = -\Gamma_A - \Gamma_C - \Gamma_E + \Gamma_G + \Gamma_H + \Gamma_I + \Gamma_L + \Gamma_O - \Gamma_R + \Gamma_S + \Gamma_U, \quad (9a)$$

$$\dot{N}_{\text{BH}} = -\Gamma_B - \Gamma_D - \Gamma_F - \Gamma_G - \Gamma_H + \Gamma_K + \Gamma_N + \Gamma_Q - \Gamma_S - \Gamma_T + \Gamma_W, \quad (9b)$$

$$\dot{N}_{\text{BH}'} = +F_{\text{gw}}\Gamma_{\text{BH+BH}} - \Gamma_I - \Gamma_J - \Gamma_K - \Gamma_L - \Gamma_M - \Gamma_N - \Gamma_O - \Gamma_P - \Gamma_Q - \Gamma_U - \Gamma_V - \Gamma_W, \quad (9c)$$

$$\dot{N}_{\text{LMGO-STAR}} = +\Gamma_A - \Gamma_C - \Gamma_D - \Gamma_J - \Gamma_L, \quad (9d)$$

$$\dot{N}_{\text{BH-STAR}} = +\Gamma_B - \Gamma_E - \Gamma_F - \Gamma_N - \Gamma_P, \quad (9e)$$

$$\dot{N}_{\text{BH}'-STAR} = +\Gamma_L + \Gamma_M + \Gamma_N - \Gamma_R - \Gamma_V - \Gamma_T, \quad (9f)$$

$$\dot{N}_{\text{BH-LMGO}} = +\Gamma_D + \Gamma_E + \Gamma_G - \Gamma_H - \Gamma_K - \Gamma_O - \Gamma_{\text{BH+LMGO}}, \quad (9g)$$

$$\dot{N}_{\text{LMGO-LMGO}} = +\Gamma_C - \Gamma_G - \Gamma_I - \Gamma_{\text{LMGO+LMGO}}, \quad (9h)$$

$$\dot{N}_{\text{BH-BH}} = +\Gamma_F + \Gamma_H - \Gamma_Q - \Gamma_{\text{BH+BH}}, \quad (9i)$$

$$\dot{N}_{\text{BH}'-LMGO} = +\Gamma_I + \Gamma_J + \Gamma_K + \Gamma_R - \Gamma_S - \Gamma_U - \Gamma_{\text{BH}'+\text{LMGO}}, \quad (9j)$$

$$\dot{N}_{\text{BH}'-BH} = +\Gamma_O + \Gamma_P + \Gamma_Q + \Gamma_S + \Gamma_T - \Gamma_W - \Gamma_{\text{BH}'+\text{BH}}, \quad (9k)$$

$$\dot{N}_{\text{BH}'-BH'} = +\Gamma_U + \Gamma_V + \Gamma_W - \Gamma_{\text{BH}'+\text{BH}'} . \quad (9l)$$

The overdots denote time derivative. This is a stiff problem and we employ backward differentiation formula methods to numerically solve it. We implement the FORTRAN package ODEPACK [68]. We note that for the binaries containing two compact objects i.e. the ones described by Eq. 9g-9l, we evolve their SMA axis to account for their 3rd-body hardening interactions. The total number of such binaries at any time is given by the sum over all values of SMAs. For instance, for the BH-LMGO binaries  $N_{\text{BH-LMGO}} = \sum_{i=1}^{100} N_{\text{BH-LMGO}}^{[i]}$  terms over the SMA bins. Also, both the hard interaction rate of Eq. 7 and the exchange cross-section (see discussion in IID), affecting the relevant exchange rate are evaluated including all 100 values of SMAs. Eqs. 9d-9f do not have SMA binning as 3rd-body interactions with other stars do not result in the binaries hardening. Nevertheless, tracking the evolving number of BH-star and LMGO-star pairs is essential as these are intermediate states towards the more interesting compact object binaries.

For the initial conditions of the differential system of Eqs. 9a-9l we take all BHs and LMGOs to be single objects. We consider each population to be uniformly distributed within their segregation volume. We discuss the evaluation of segregation volumes for different compact objects in Appendix A. The integration of the differential equations is proceeded along the segregation volume of the BHs,  $V_{\text{BH}}$  because the BHs can only interact with the LMGOs in the intersection region of their segrega-

tion volumes. Subsequent interactions of these compact objects with star-star binaries will induce pairs including BHs and LMGOs through a cascade exchange processes as in Fig. 1. We also note that when compact objects are replaced by more massive ones through exchanges (as e.g. in channels “G” of “H” for LMGOs), those objects are taken to remain inside the cluster. We have estimated that their velocity after the exchange is still smaller than the typical escape velocity from the globular clusters.

The number of star-star binaries is an initial condition in this work. These could be protobinaries<sup>2</sup> or could have been assembled via three body induced mechanism. To parametrize the number of star-star pairs in the core of a given globular cluster we take the number density of stars in the core as  $n_{\text{star}} = \frac{\rho_0}{m_*}$ . The symbol  $\rho_0$  is the central mass density of the cluster obtained directly from the globular cluster Harris catalog [2]. We take a fraction  $f_{\text{bin}}$  of these stars to participate in star-star binaries and of them only a fraction  $f_{\text{hard}}$  to be in hard binaries. Therefore, the number density of hard star-star pairs is given by  $n_{\text{star-star}} = \frac{1}{2} f_{\text{hard}} f_{\text{bin}} n_{\text{star}}$  with typical value for  $f_{\text{hard}} \cdot f_{\text{bin}} = 0.05$ . We take that to be our choice in this work. We probe the effect this fraction has on our results in Appendix B. The total number of these binaries inside the segregation volume of the BHs

<sup>2</sup> By the term “protobinary” here we mean a binary that was created when the cluster was form.

is equal to  $N_{\text{star-star}} = n_{\text{star-star}} V_{\text{BH}}$ . Furthermore, we do not evolve the number of star-star binaries, as their number is far greater than that of the compact objects and essentially constant.

We have included “attenuation” terms for the LMGO-LMGO, BH-LMGO, BH'-LMGO, BH-BH, BH'-BH and BH'-BH' binaries that represent their mergers. These terms correspond to the coalescence of hard binaries through the process of hardening by 3rd-body interactions with stars [4]. Given a type A-B binaries inside a cluster of number  $N_{A-B}$ , their merger rate is going to be,

$$\Gamma_{A+B}(t) = N_{A-B}^{a=a_{\text{GW A-B}}}(t)/T_{\text{GW A-B}}, \quad (10)$$

which evolves with time as the number of binaries of type A-B with a SMA of  $a = a_{\text{GW A-B}}$ ,  $N_{A-B}^{a=a_{\text{GW A-B}}}$  evolves with time as well.

$$f(m_1, m_2, m_3) = \frac{m_3^{7/2}(m_2 + m_3)^{1/6}}{(m_1 + m_2)^{1/3}(m_1 + m_3)^{5/2}(m_1 + m_2 + m_3)^{5/6}} \times \exp(3.70 + 7.49x - 1.89y - 15.49x^2 - 2.93xy - 2.92y^2 + 3.07x^3 + 13.15x^2y - 5.23xy^2 + 3.12y^3), \quad (12)$$

with  $x = m_1/(m_1 + m_2)$ ,  $y = m_3/(m_1 + m_2 + m_3)$  and valid within the point-mass approximation.

The corresponding velocity averaged exchange rate density for  $1-2 \rightarrow 3-2$ , assuming a Maxwell-Boltzmann distribution for the relative velocity, is given by,

$$\gamma_{\text{ex}} = \sqrt{\frac{6}{\pi}} n_{1-2} n_3 \frac{G(m_1 + m_2 + m_3)a}{\sigma_{3,1-2}} \times f(m_1, m_2, m_3). \quad (13)$$

The number densities  $n_{1-2}$  and  $n_3$  depend on the radial position inside the cluster. The exchange rates that enter Eqs. 9a-9l, are just,

$$\Gamma_{\text{ex}} = \int \gamma_{\text{ex}} dV = \gamma_{\text{ex}} \times \min(V_{1-2}, V_3). \quad (14)$$

The integration is done over the portion of volume of the cluster where  $1-2 \rightarrow 3-2$  exchanges occur. We consider the  $1-2$  and  $3$  to be distributed uniformly within their respective segregation volumes  $V_{1-2}$  and  $V_3$ .

In Fig. 2 we show  $f(m_1, m_2, m_3)$  for certain choices of masses. We note that the exchange process  $1-2 \rightarrow 3-2$  has a high probability of occurring as the third object approaching the binary has a mass larger than both of the binary components. On the other hand, if  $m_3 < \min(m_1, m_2)$  the cross section drops and the probability of exchange becomes essentially zero when the  $m_3 < m_1/\sqrt{10}$ . Furthermore, there is a strong dependence between the mass of the intruder and of the exchanged object, while a weak dependence on the mass of the remained object. Therefore, since the mass of stars

#### D. Binary-single exchange cross section and exchange rates

The exchange cross section for an object of mass  $m_3$  to substitute an object of mass  $m_1$  in a hard binary system  $1-2$  is given by,

$$\Sigma_{\text{ex}} = \frac{G(m_1 + m_2 + m_3)a}{v_{3,1-2}^2} \times f(m_1, m_2, m_3). \quad (11)$$

$a$  here is the SMA of  $1-2$  before the exchange and  $v_{3,1-2}$  the relative velocity of object  $3$  to the binary calculated at infinity. As the  $1-2$  is a hard binary the exchange cross section contains only the gravitational focusing term. This is averaged over orbital eccentricities following a thermal distribution  $P(e)de = 2ede$ . The form factor,  $f(m_1, m_2, m_3)$  is equal to [69],

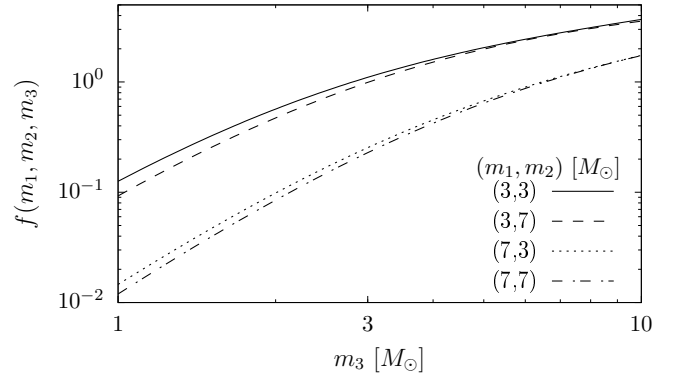


FIG. 2. The form factor  $f(m_1, m_2, m_3)$  as a function of the third mass  $m_3$  and for four choices of binary masses  $(m_1, m_2)$ . It is assumed that the  $m_1$  is exchanged by  $m_3$ .

is typically  $m_* < 1M_\odot$ , and the masses of BHs and LMGOs is greater than  $3M_\odot$ , we neglect exchanges in which a star substitutes an LMGO or a BH.

#### E. The impact of second generation black holes

We consider the situation in which a pair of first generation black holes BH of mass  $10 M_\odot$  each coalesces to give a second generation black hole BH' with a mass of  $19 M_\odot$ . In realistic situations where the masses of the merging BHs are not equal, the product BH' obtains

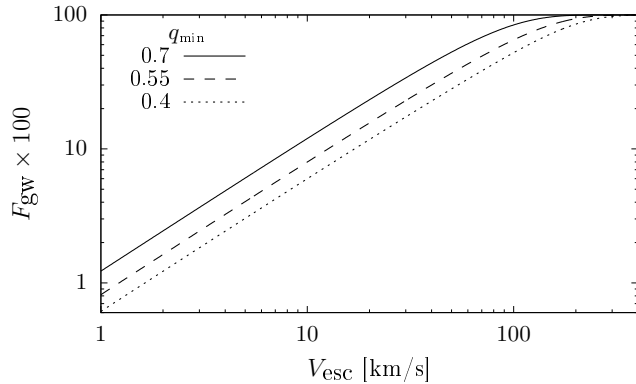


FIG. 3. The retention fraction of second generation BH' merger remnants as a function of the escape velocity from their host cluster and under the assumption of a uniform mass ratio distribution. The lines are for three values of the smaller mass ratio  $q_{\min}$ . The labels denote the value of  $q_{\min}$ .

a GW kick and may escape from the cluster. In Appendix C we describe in full detail how we treat this kick and how we calculate the fraction of the retained BH' in each globular cluster.

We find that the retention fraction of second generation BH' in a cluster with escape velocity of 50 km/s (a typical value for large GCs), is approximately 20%. For an escape velocity above 400 km/s the fraction saturates to 100%. In Fig. 3 we show the retention fraction  $F_{\text{gw}}$  for BH' objects versus the escape velocity from a cluster. The  $q_{\min}$  refers to the minimum value of mass ratio between the merging first generation black holes for a realistic BH mass spectrum. The  $q_{\min} = 0.55$  curve that is also our reference choice gives a rough estimate of the retention fraction of second generation black holes, which we find that can be parametrized well as,

$$F_{\text{gw}}(V_{\text{esc}}) \simeq \left( \frac{V_{\text{esc}}}{1.2 \text{ km/s}} \right)^{0.97} \% , \text{ for } V_{\text{esc}} < 100 \text{ km/s}. \quad (15)$$

This relation holds true to within a few percent for the vast majority of Milky Way type GCs.

The total retention fraction in Eq. 15 controls the amount of second generation black holes BH', which remain in the cluster and are imported in our Fig. 1. The corresponding creation rate of BH' is  $F_{\text{gw}} \times \Gamma_{\text{BH+BH}}$ , where  $\Gamma_{\text{BH+BH}}$  is the merger rate of BH-BH pairs.

### III. RESULTS

The solution of the differential system in Eqs. 9a-9l, yields the time evolution of the population sizes inside  $V_{\text{BH}}$ . In this section we present the results of this model.

#### A. The depletion of BHs and LMGOs

Single BHs and LMGOs first create binaries with stars which then they exchange with more massive objects. While single BHs are more numerous than the LMGOs, due to their larger mass their numbers deplete faster. LMGOs create stable binaries with other LMGOs or BHs when the number of single BHs is significantly reduced. Processes like “H” in Fig. 1 in which a BH-LMGO pair becomes a BH-BH pair and an LMGO is freed decelerates somewhat the rate by which the population of single LMGO depletes. This also explains why BH-BH mergers grow in numbers earlier than mergers involving an LMGO. BHs tend to coalesce with LMGOs in the late stages of a cluster after the binary BH population has settled down.

#### B. The formation of BH-LMGO binaries inside globular clusters

Binaries of first generation black holes BH with low mass gap objects are a class of binary systems that form dynamically inside clusters. These binaries are seeded from three binary populations, LMGO-star pairs from channel “D”, BH-star pairs from channel “E” and LMGO-LMGO pairs via channel “G” (see Fig. 1). However, they can also be depleted by exchange interactions with first generation black holes via channel “H” or when second generation black holes BH' are formed and cause exchange interactions “K” and “O”. In Fig. 4, we show the evolution with time of those rates (left panel) as the number of each of the individual objects and of the binaries involved changes with time. We use the environmental parameters of Terzan 5 globular cluster to produce these lines. Solid lines represent positive rate terms increasing the number of BH-LMGO binaries and dashed lines negative terms reducing it.

The two main pathways in the formation of BH-LMGO pairs are the formation first of BH-star pairs, followed by the exchange of the star with a single LMGO ( $B \rightarrow E \rightarrow \text{BH-LMGO}$ ) and the formation of a LMGO-star pair first, followed by an exchange interaction with a BH ( $A \rightarrow D \rightarrow \text{BH-LMGO}$ )<sup>3</sup>. Channel G is very rare as there aren't many LMGO-LMGO pairs in the first place. Even though, there are many ways to form a BH-LMGO binary, their numbers inside clusters are small. It is difficult to form single LMGOs. Also, many of these objects are at orbits inside the cluster but beyond the core dominated by BHs and do not interact with them. These prove more important factors in the suppression of the rates of BH-LMGO formed, compared to the occasional exchange interactions the BH-LMGO binaries can have with other

<sup>3</sup> We assume that LMGO-star interactions with BHs always lead to the creation of a BH-LMGO pair and not to BH-star ones.

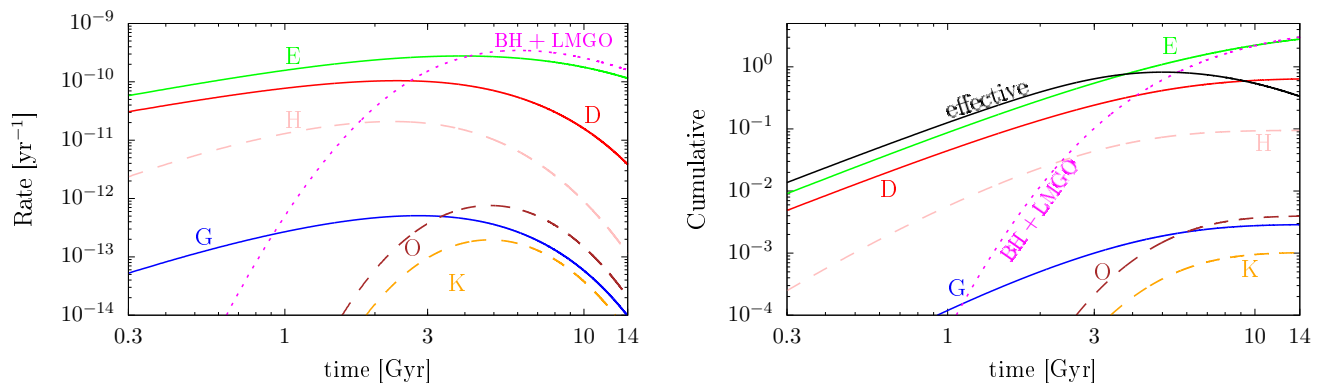


FIG. 4. *Left panel:* The exchange and merger rates associated with the BH-LMGO binaries (see Fig. 1). Solid lines represent exchange channels that increase the number of BH-LMGO binaries inside the cluster and dashed lines channels reducing it via exchanges. *Right panel:* The corresponding cumulative number of BH-LMGO pairs created or annihilated in the history of the cluster as well as the effective number of BH-LMGO pairs as a function of time. The black line denoted as “effective” shows the evolution of the number of BH-LMGO binaries. To produce these curves we used the properties of Terzan 5 globular cluster.

black holes leading to LMGOs getting replaced by first or second generation black holes (dashed lines in Fig. 4). In the right panel of Fig. 4, we show the cumulative number of BH-LMGO binaries formed over time from each specific channel (in solid lines) and also the cumulative number of BH-LMGO binaries destroyed by exchanges with black holes from each specific channel (in dashed lines).

In addition, in Fig. 4, we present the evolution with time of the total BH-LMGO merger rate and number of BH-LMGO mergers inside Terzan 5 (dotted lines at the left and right panels respectively). We allow those numbers to be non-integers as we will later present calculations involving other Milky Way cluster environments and will sum the contribution from many clusters to evaluate their typical averaged contribution to the total rates of BH-LMGO mergers in the Universe. Toward the end of the cluster’s history presented, the number of BH-LMGO pairs (line denoted as “effective”) drops as mergers occur.

Since second generation black holes BH’ coming from the BH-BH mergers are formed inside the clusters, we also include their impact both in disrupting BH-LMGO binaries but also in creating the more rare BH’-LMGO pairs, i.e. binaries where the black hole is a second generation one. Those are presented in Fig. 5. We follow the same notation as for Fig. 4, where positive rates for the formation of such binaries come from channels “T”, “J”, “K” and “R”, and negative disruption rates due to exchanges of LMGOs by more massive black holes from channels “S” and “U”. The number of BH’-LMGO binaries is dominated by the number of LMGO-stars having exchange interactions with BH’ objects ( $A \rightarrow J \rightarrow \text{BH}'\text{-LMGO}$ ) and by BH’-star binaries having exchange interactions with single LMGOs ( $M \rightarrow R \rightarrow \text{BH}'\text{-LMGO}$ ). However, we find that such binaries are far less common to exist and merge by about a factor of  $\sim 30$ , as second generation black holes are far rarer. If their number inside dense stellar environments is enhanced so will their

respective binaries.

In Fig. 6, we show the evolution of the numbers of single compact objects LMGO, BH and BH’ as well as the evolution of number of those compact objects with each other and with stars inside Terzan 5 globular cluster. For each binary type and for each type of interaction effecting those numbers we have taken into account the relevant segregation volumes of the objects involved as described in Eqs. 8 and 14. As can be seen the formation of BH-LMGO binaries is somewhat delayed by comparison to BH-BH as LMGOs can be replaced by BHs via exchanges. Most single BHs are in BH-star and BH-BH pairs. Only after most BHs are in these binaries the number of BH-LMGO binaries peaks. LMGO-LMGO binaries are even more rare and require for the number of single BHs to be very suppressed before they can remain in stable binaries that can then harden via 3rd-body interactions with stars.

BH’-LMGO systems are delayed due to the required merger of  $\text{BH} + \text{BH} \rightarrow \text{BH}'$ . Yet, once those second generation black holes are produced, the relevant cross-section for them to interact with other binaries is so large that binaries with a BH’ as a member form very fast as seen by the rapidly increasing cyan (BH’-star), rose (BH’-BH), pastel (BH’-LMGO) and green (BH’-BH’) lines.

### C. The formation of black hole binaries with a second generation black hole

In Fig. 6, we also present the binaries formed containing a first generation and a second generation black hole. Those are created via the channels “O”, “P”, “Q”, “S” and “T” of Fig. 1 and are reduced just when a second BH’ replaces the first generation black hole (channel “W”). In Fig. 7, we show the evolution of those rates and of the relevant cumulative numbers. The most important channels are those involving the binaries containing a star



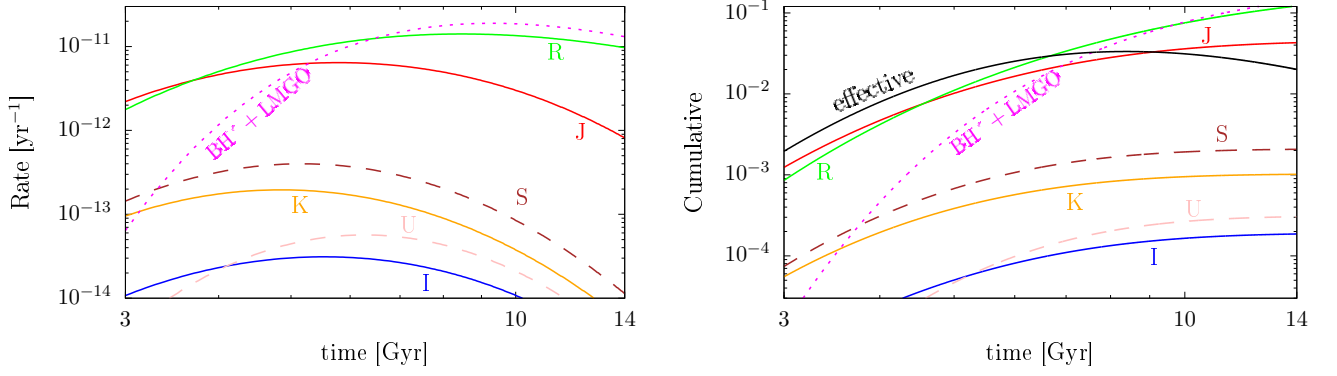


FIG. 5. *Left panel:* The exchange and merger rates associated with the BH'-LMGO binaries (see Fig. 1). *Right panel:* The corresponding cumulative number of BH'-LMGO pairs created or disrupted in the history of the Terzan 5 cluster as well as the effective number of BH'-LMGO pairs as a function of time.

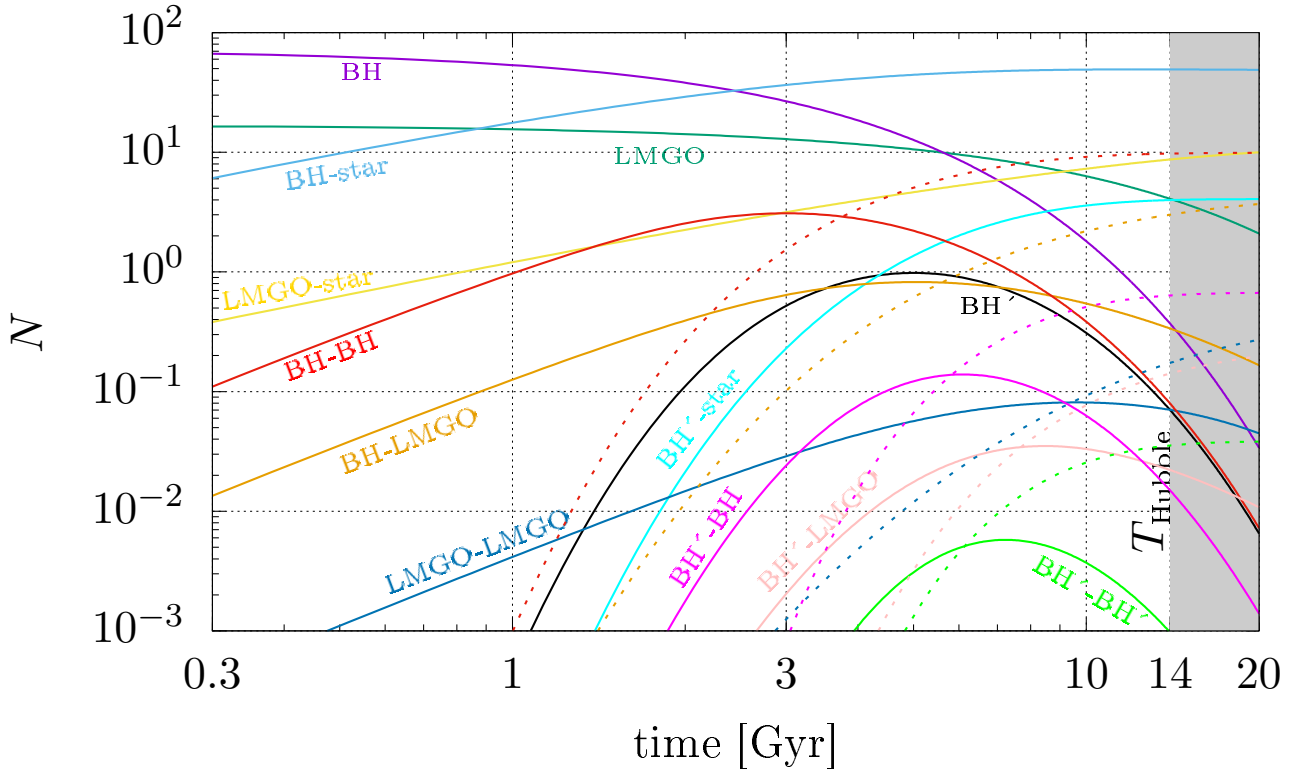


FIG. 6. The time evolution of all single compact objects (LMGO, BH, BH') and binary types that we consider in our model (Fig. 1) as well as their corresponding cumulative number of mergers in dotted lines. These numerical results have been obtained in the core of our reference cluster Terzan 5. The gray shaded region represents the region to the right of Hubble time which is taken to be 14Gyr.

and a black hole which is then replaced by a second black hole, (B  $\rightarrow$  P  $\rightarrow$  BH'-BH and M  $\rightarrow$  T  $\rightarrow$  BH'-BH).

While rare, these binaries still lead to BH'-BH mergers that are only about a factor of  $\simeq 30$  less common than the regular BH-BH merger events, i.e. two first generation black holes merging and thus can provide a detectable rate of events.

#### D. Build-up of the LMGO population

A major assumption that we made in the above mentioned results is that there is an initial number of LMGOs inside the cluster that can dynamically interact with other objects already in the first time-step. Unlike first generation BHs that form in the very first  $\sim 10$  million years of the clusters's existence, LMGOs depending on

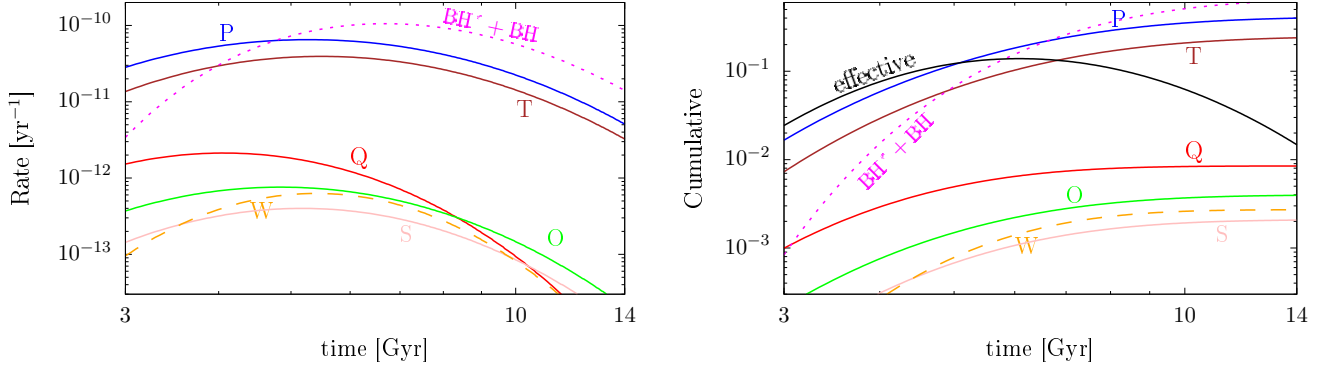


FIG. 7. *Left panel:* The exchange and merger rates associated with the BH'-BH binaries (see Fig. 1). *Right panel:* The corresponding cumulative number of BH'-BH pairs created or annihilated in the history of Terzan 5 as well as the effective number of BH'-BH pairs as a function of time.

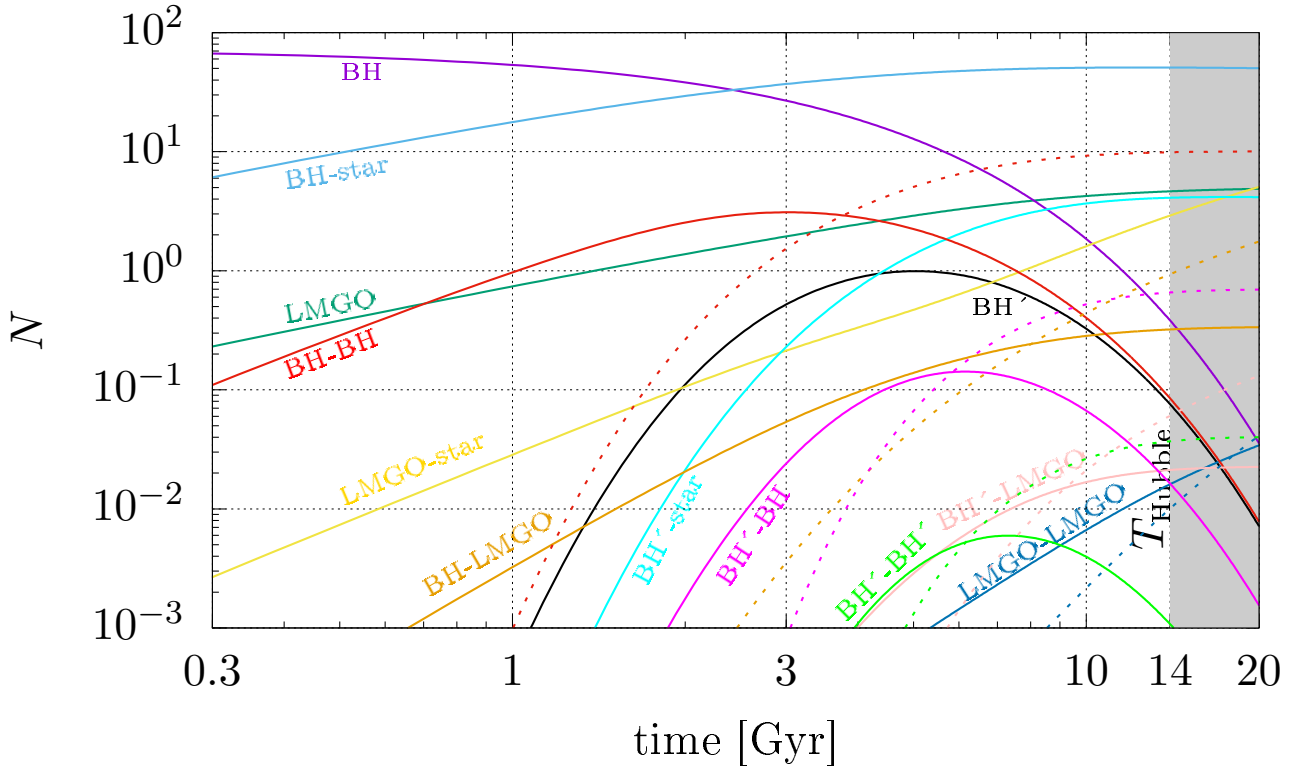


FIG. 8. As in Figure 6 but for a population of LMGOs that gradually builds up (solid green line). The time evolution of all single compact objects and binary types considered in this work is shown in solid lines. In dotted lines we show the corresponding cumulative number of mergers.

their origin may require much longer time to form. In this section instead, we make the assumption that the population of  $3M_{\odot}$  LMGOs is created via NS-NS mergers inside the GCs and there is a gradual build-up of the LMGO's population. We take the initial population of LMGOs to be zero,  $N_{\text{LMGO}}(t=0) = 0$  and consider a source term into the equation for the evolution of LMGOs represented by the NS+NS merger rate. Specifically, we

rewrite Equation 9a adding the relevant source term,

$$\dot{N}_{\text{LMGO}} = F_{\text{gw}}\Gamma_{\text{NS+NS}} - \Gamma_{\text{A}} - \Gamma_{\text{C}} - \Gamma_{\text{E}} + \Gamma_{\text{G}} + \Gamma_{\text{H}} + \Gamma_{\text{I}} + \Gamma_{\text{L}} + \Gamma_{\text{O}} - \Gamma_{\text{R}} + \Gamma_{\text{S}} + \Gamma_{\text{U}}, \quad (16)$$

$F_{\text{gw}}$  is taken to be 1 and thus the source term is,

$$\Gamma_{\text{NS+NS}}(t) = N(t)\Theta(N(t))\Theta(T_{\text{Hub}} - t)\frac{f_e(T_{\text{Hub}} - t)}{T_{\text{Hub}} - t} \quad (17)$$

where  $T_{\text{Hub}}$  is the Hubble time,  $\Theta$  is the Heaviside function and  $N(t) = (N_{\text{NS}}/2 - N_{\text{LMGO}}(t))$  is the number of NS-NS hard pairs at time  $t$ .

We point out that for this work the time  $t = 0$  is the moment that both the first generation of BHs and the  $1 M_{\odot}$  stars have been formed and exist in binaries inside the cluster. We also assume that the segregation of BHs in the cluster's core has taken place.  $1 M_{\odot}$  stars still require  $\simeq 40$  Myrs to form from contraction of their initial gas clouds and thus follow the formation of first generation BHs which only require  $O(10)$  Myrs altogether. The segregation of BHs inside the core also requires  $O(10)$  Myrs. All these are significantly smaller timescales compared to the exchange ones at  $t \simeq 0$ . Thus exchanges happen after those phases in the history of a cluster have taken place.

In Fig. 8, we show the cumulative number of compact objects, their binaries and of merger events for Terzan 5 as they all evolve. This can be compared to Figure 6 that did not include the gradual build-up of LMGOs. With the obvious exception of changing the number of binaries containing LMGOs, the effect of a gradual built up of LMGOs is entirely insignificant for all the other types of binaries. All channels in Fig. 1 and Equations 9a-9l describing LMGOs have a very small effect on the evolution of non-LMGO binaries.

We point out that, even after including this major change on the initial conditions of the LMGOs number, the number of BH-LMGO and the BH'-LMGOs mergers in the history of the cluster is only suppressed by a factor of four and two respectively compared to the case where we included LMGOs from the first time-step. The time-demanding build-up included in this section represents a slow pathway in the creation of LMGOs and our results in section III B an "instant" one. Thus in combination our results provide a wide width of possibilities. Our results of modeling the dynamical interactions of LMGOs with other objects inside dense stellar clusters are quite generic and independent to the exact origin of the LMGOs. As long as their number in a stellar environment does not exceed that of first generation BHs our results can be applicable to wide range of possible explanations on the BH-LMGO events as GW190814.

### E. Average Cumulative Cases and merger rates

In Figs. 4 to 8 we used for reference Terzan 5 cluster as it is a massive one that can contain significant numbers of BH, BH' and LMGOs. While Terzan 5 is an instructive example, we care for the averaged rate of mergers in globular clusters. For that we use the 106 Milky Way clusters for which we have reliable data of their mass profile. Those rejected are the smallest mass ones,

We evaluate the average cumulative number of mergers per cluster for the six binary species we consider, i.e. BH-LMGO, LMGO-LMGO, BH-BH, BH'-LMGO, BH'-BH and BH'-BH'. While in the Figs. 4 to 8 we plotted

results all the way to the Hubble time, the typical age of cluster is a few Gyrs smaller. For that reason we calculate the cumulative number of mergers at 10 Gyr of evolution time. In Table I, we show the expected number of mergers in the history of a variety of Milky Way clusters for each type of binary. Also, (at the last line) we give the average number of mergers per cluster. We assume no delay in the initial population of LMGOs.

BH-BH mergers provide the most abundant class of mergers in globular clusters. Such binaries are build from BH-LMGO and BH-star binary exchange interactions with single BHs. They are also well measured by LIGO-Virgo and can provide a reference for the more exotic channels. In terms of rates we get that there are  $5.7 \times 10^{-11} \text{ yr}^{-1}$  per cluster BH-LMGO mergers and  $1.8 \times 10^{-12} \text{ yr}^{-1}$  per cluster BH'-LMGO mergers. By comparison, for BH-BH mergers which constitute the majority of LIGO's binary black hole merger events, we get  $4.3 \times 10^{-10} \text{ yr}^{-1}$  per cluster mergers. We do find though that globular clusters can give  $2.0 \times 10^{-11} \text{ yr}^{-1}$  BH'-BH and  $1.3 \times 10^{-12} \text{ yr}^{-1}$  per cluster BH'-BH' mergers. Such rates allow for LIGO-Virgo to see both BH-LMGO and BH'-BH in a small sample of its events, as it may already have with GW190814 for the BH-LMGO case. We also find a rate of  $1.9 \times 10^{-12} \text{ yr}^{-1}$  per cluster for LMGO-LMGO binaries which we expect will be observable events as the LIGO-Virgo sensitivity develops.

To get a conservative estimate for local BH-LMGO binary merger rate, we take the local number density of globular clusters to be constant at  $n_{GC}(z) = 0.77 \times 10^9 \text{ Gpc}^{-3}$  [5]. We also allow for an evolving with redshift globular cluster density, as  $n_{GC}(z) = 0.77 \times 10^9 \cdot E(z)^3 \text{ Gpc}^{-3}$  <sup>4</sup>. Assuming the Milky Way sample to be representative of the averaged local Universe up to redshift  $z$  of 1, we estimate the cumulative merger rate  $\mathcal{R}_c(z = 1)$  [5, 71],

$$\mathcal{R}_c(z = 1) = \int_0^{z=1} dz' \langle \Gamma_{GC}(z') \rangle n_{GC} \frac{dV_c}{dz'} (1 + z')^{-1}. \quad (18)$$

where  $V_c$  is the comoving volume. We get a merger rate density of  $\Gamma_{\text{BH-LMGO}} = \mathcal{R}_c(z = 1)/V(z = 1) \simeq (2 - 8) \times 10^{-2} \text{ Gpc}^{-3} \text{ yr}^{-1}$ . If instead, we use the hypothesis that the number of LMGOs was build-up via NS-NS mergers then that rate density becomes  $\Gamma_{\text{BH-LMGO}} \simeq (0.4 - 1.3) \times 10^{-2} \text{ Gpc}^{-3} \text{ yr}^{-1}$ . By comparison, the experimentally inferred merger rate density of GW190814-like events is  $(1 - 23) \text{ Gpc}^{-3} \text{ yr}^{-1}$ . Our predicted rates tend to be lower by an order of magnitude compared to the LIGO-Virgo values. As we pointed out if more LMGOs are produced via a non-NS channel, those rates will be enhanced. Also, other environments as nuclear clusters in galaxies whose population properties are less well-understood, could enhance the BH-LMGO merger

<sup>4</sup>  $E(z) = \sqrt{\Omega_M \cdot (1 + z)^3 + \Omega_\Lambda}$ , with  $\Omega_M = 0.3$  and  $\Omega_\Lambda = 0.7$ , based on Planck data (2015) [70].

GC	$N_{\text{BH}}^{\text{init.}}$	$N_{\text{LMGO}}^{\text{init.}}(V_{\text{BH}})$	BH+LMGO	LMGO+LMGO	BH+BH	BH'+LMGO	BH'+BH	BH'+BH'
				$\times 10^{-2}$		$\times 10^{-2}$	$\times 10^{-1}$	$\times 10^{-2}$
Terzan 5	73	16	2.19	9.24	9.15	6.36	4.22	1.75
NGC 104	499	109	4.03	6.90	44.0	2.30	7.88	2.08
NGC 1851	82	18	2.31	8.86	10.6	5.98	4.77	2.02
NGC 6266	415	105	6.18	15.1	51.4	16.1	24.9	12.6
NGC 6293	11	2	0.44	3.24	1.19	0.845	0.258	0.07
NGC 6440	119	29	3.71	18.1	16.4	12.7	9.85	4.86
NGC 6441	788	208	12.8	45.5	106	45.7	65.8	45.2
NGC 6522	9	1	0.395	2.91	1.08	0.767	0.233	0.07
NGC 6624	8	1	0.251	1.87	0.654	0.368	0.112	0.02
NGC 6626	99	21	1.67	5.49	12.2	2.86	3.66	1.31
NGC 6681	9	1	4.62	3.42	1.30	0.115	0.347	0.14
NGC 7078	540	122	64.7	13.2	64.4	1.24	25.2	11.3
average	82	21	0.57	1.9	4.3	1.8	2.0	1.3

TABLE I. The cumulative number of mergers for each of the six binary species at 10 Gyr of evolution. In the first 12 rows present the clusters with the highest contribution. The last row shows the average cumulative number of mergers averaged over the ensemble of 106 Milky Way globular clusters.

rate density. If the retention fractions of BHs and NSs are increased by similar factors, then all the merger rates would grow, while the ratio of between the different types of merger events would stay approximately the same.

We point out that in the rates mentioned here, we took the averaged over 10 Gyr rates from the 106 Milky Way globular clusters as being constant. That is an approximation that underestimates the rates at lower redshifts. Each cluster requires some time for the dynamical interactions to take place. Thus, there are very few mergers in the first Gyrs in most cluster's history, while those rates increase significantly at the last few Gyrs (see e.g. Fig. 6). Each cluster due to its own density and mass has each own history of mergers. Small dense clusters evolve rapidly while more massive ones produce mergers later due to their smaller central densities (as 47Tuc). This is shown in Fig. 9 where we give the number of cumulative mergers and the equivalent rate per cluster.

While we can not directly assume the exact same evolution histories for globular clusters in other galaxies, Fig. 9 allows us to include the redshift evolution of the BH-LMGO mergers inside globular clusters (calculated in per cluster units). Assuming no build-up on the LMGO number we get a total merger rate density of  $\Gamma_{\text{BH-LMGO}} \simeq (5 - 16) \times 10^{-2} \text{Gpc}^{-3} \text{yr}^{-1}$ . The main effect of that correction is the larger by a factor of two rate density. This is a direct result of the dominant contribution from massive globular clusters at late times.

#### IV. CONCLUSIONS AND DISCUSSION

In this work we modeled the mechanism through which compact binaries, involving low-mass gap objects and/or black holes, form via exchange interactions inside Milky Way globular clusters. The formed compact object binaries undergo hardening via interactions with stars in the same environments leading to their accelerated merger. Our basic scheme of interactions is depicted in Fig. 1.

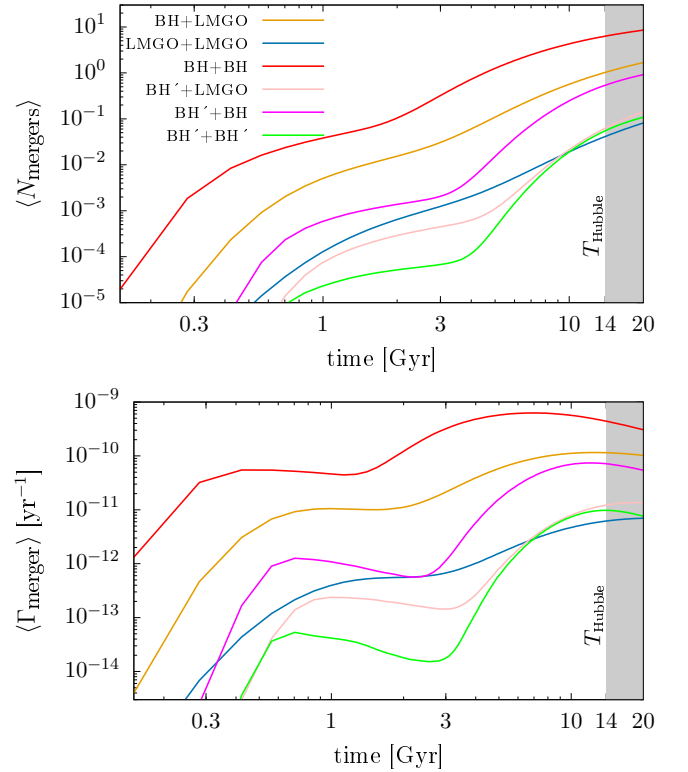


FIG. 9. Globular clusters dominating in different epochs. There is a contribution coming from dense small clusters which evolve rapidly as M30. Later a more dominant contribution comes from the larger clusters that evolve slower. *Top*: cumulative number per cluster, *bottom*, averaged merger rate per cluster. We use the same color coding in both panels.

For simplicity, we took monochromatic mass spectra for both the LMGOs, the first generation black holes and the stars. We also included second generation black holes which result from merging first generation black hole bi-

naries. Those second generation black holes can affect the dynamics inside the clusters and the merger rates of compact object binaries as those including LMGOs. We took for the LMGOs number inside globular clusters to be directly related to the number of neutron stars that remain in those environments after their initial natal kick. We calculate the merger events for each type of binary using the observed Milky Way globular clusters from Ref. [2]. We rely on their observed total mass and mass profile properties. In Fig. 6, we show for the Terzan 5 globular cluster the cumulative number of merger events and the evolution of the populations of individual compact objects and of binaries containing compact objects. From the Milky Way sample we then evaluated the averaged merger rates per cluster for each of the binary compact objects types, shown in Table I.

We have found that the merger rate density of BH-LMGO mergers in the local Universe to be in the range  $0.004 - 0.16 \text{ Gpc}^{-3} \text{ yr}^{-1}$  up to a redshift of  $z = 1$ . This result's range is associated mostly to how fast the LMGOs formed in the history of those clusters. This value is below the inferred rate from the GW190814 event i.e.  $1-23 \text{ Gpc}^{-3} \text{ yr}^{-1}$  but provides a lower estimate for these type of events. Thus globular clusters as set of environments can provide a population of such merger events. Depending on the individual cluster's mass profile and total mass, different types of clusters contribute at different epochs, with the more massive ones dominating the total number of merger events at low redshifts (see Fig. 7).

We do not evolve binaries involving stars, but rather monitor their population sizes. Furthermore, we do not evolve the stellar cluster in time but instead integrate the evolution equations inside the volume in which the black holes uniformly populate, ignoring the possible existence of a massive BH at the center of the cluster. The spin of compact objects was not taken into account, as analysis of the observed mergers suggests that black holes tend to have very small spins that are narrowly distributed [72, 73]. We have calculated the contribution to the merger rates from direct capture events, i.e. hard compact object binaries forming from strong dynamical encounters of individual objects and find it to be insignificant<sup>5</sup>.

Three-body induced binaries involving compact objects are rare and typically form soft pairs that do not survive long enough inside the clusters. Thus we ignore them. We expect that binary-binary interactions can be of some importance in the evolution history of the clusters with the highest central densities (see e.g. [74, 75]). However, the total BH-LMGO, BH'-LMGO, BH-BH and BH'-BH merger rates are dominated by the most massive

clusters, for which the binary-binary interactions only now (at  $t \simeq 10 \text{ Gyr}$ ) start having an impact. We leave that higher order correction in our calculations for future work, pointing out that it would only increase the claimed merger rates.

The origin of the LMGOs is of importance. They represent a new category of objects with their own mass spectrum in the low mass region and could be of exotic origin as primordial black holes formed in the early Universe. Here to be conservative we assumed that their totality is accounted for by the NS-NS mergers. Thus, our work provides a realistic lower estimate of the BH-LMGO merger rate inside globular clusters. We have focused on the impact this population has on the dynamics and formation of binaries involving at least one LMGO; leaving their origin as an open question.

*Acknowledgements:* The authors are grateful to A. Kehagias for his support in facilitating this collaboration. IC acknowledges the Faculty Research Fellowship support from the Oakland University Research Committee.

## Appendix A: Velocities and segregation radii

According to the Virial theorem the three dimensional velocity dispersion of stars is given by  $\sigma_* = \sqrt{\frac{3}{5} \frac{GM_{\text{cl}}}{r_h}}$ , where  $M_{\text{cl}}$  is the mass of the cluster and  $r_h$  is the half-mass radius<sup>6</sup>. In this context, stars represent the mean mass population,  $\langle m \rangle = m_*$  as they are the most abundant objects in any globular cluster. Taking into account the fact that energy equipartition is not necessarily achieved in stellar clusters, [76, 77], the velocity of massive species with mass  $m$  is given by  $\sigma(m) = \left(\frac{m}{2m_*}\right)^{-0.16} \sigma_*$  [77]. The relative velocity dispersion between two populations with masses  $m_1$  and  $m_2$  is given by,

$$\sigma_{1,2} = \sqrt{\sigma_1^2 + \sigma_2^2} = \sqrt{\frac{m_1^{-0.32} + m_2^{-0.32}}{(2m_*)^{-0.32}}} \sigma_*. \quad (\text{A1})$$

Massive objects through dynamical friction sink towards the cluster's core partially segregating from the stars. Applying the Virial theorem for the segregated sub-population with objects of mass  $m$ , we find its half-mass radius  $R_{\text{seg}}(m)$ . This segregation radius is obtained by solving numerically the following algebraic equation, [78],

$$\frac{4M(R_{\text{seg}}(m))}{M_{\text{cl}}} = \left(\frac{m}{2m_*}\right)^{-0.32} \frac{R_{\text{seg}}(m)}{r_h}. \quad (\text{A2})$$

<sup>5</sup> For instance, in the early stages of Terzan 5, the capture merger rate of two first generation of BHs is  $8.6 \times 10^{-13} \text{ yr}^{-1}$ . The corresponding rate for the exchange process “B” in Fig. 1 is  $2.2 \times 10^{-8} \text{ yr}^{-1}$  by comparison.

<sup>6</sup> The factor of  $3/5$  comes from integrating a uniform sphere of mass to obtain its potential and combine with scalar Virial theorem in steady state.

	BH+LMGO	BH'+LMGO	BH'+BH
		$\times 10^{-2}$	$\times 10^{-1}$
reference	0.565	1.77	2.04
$m_{\text{BH}} = 7M_{\odot}$	0.634	1.11	1.18
$m_{\text{BH}} = 13M_{\odot}$	0.553	2.38	2.49
$m_{\text{LMGO}} = 4M_{\odot}$	1.03	3.28	2.17
$m_{\text{star}} = 0.3M_{\odot}$	0.619	1.93	1.61
$H = 15$	0.482	1.25	1.21
$K = 0$	0.473	1.07	1.21
$K = 0.1$	0.770	2.99	3.19

TABLE II. The averaged cumulative number of BH-LMGO, BH'-LMGO and BH'-BH mergers per cluster at 10Gyr. The first row of data uses the reference values of  $m_{\text{BH}} = 10M_{\odot}$ ,  $m_{\text{LMGO}} = 3M_{\odot}$ ,  $m_{\text{star}} = 1M_{\odot}$ ,  $H = 20$  and  $K = 0.05$ , as in Table I. In the following rows we vary the value of a single model variable, away from its reference one.

$M(R_{\text{seg}}(m))$  is the cluster's mass up to  $R_{\text{seg}}(m)$ .  $M(R_{\text{seg}}(m))$  is simply evaluated for BHs that exist well within the core radius but is less trivial for NSs or LMGOs that occupy a larger value and mass density of the cluster has a profile. We assume the King profile for the total mass density [79]. As an example, the segregation volume of BHs with mass  $m_{\text{BH}}$  is given by  $V_{\text{BH}} = \frac{4}{3}\pi(R_{\text{seg}}(m_{\text{BH}}))^3$ .

## Appendix B: The dependence of our results on input parameters

In this work we used specific choices for the masses of the stars and compact objects to evaluate the merger rates of BH-LMGO and the other type of compact object binaries. In addition, the subsequent hardening rate for these compact object binaries from 3rd-body interactions with stars described in Eqs. 2 and 3, is set by the choice of the hardening rates  $H$  and  $K$ . In Table II, we show how our main resulting per cluster averaged merger rates for BH-LMGO, BH'-LMGO and BH'-BH binaries change with alternative choices for each of these six parameters. We remind the reader that our reference choices in the main text were,  $m_{\text{BH}} = 10M_{\odot}$ ,  $m_{\text{LMGO}} = 3M_{\odot}$ ,  $m_{\text{star}} = 1M_{\odot}$ ,  $H = 20$  and  $K = 0.05$ . The mass of a second generation black holes is derived from the choice of first generation black hole to be  $m_{\text{BH}'} = 1.9 \times m_{\text{BH}}$ , i.e  $19 M_{\odot}$  in our reference case.

We find that most alternative choices to our reference ones, affect our merger numbers and subsequent rates by only up to  $\simeq 50\%$ , with the reference ones giving the representative values. For instance, changing the mass of stars to a smaller value of  $0.3 M_{\odot}$  and the impact it has on the BH'-BH mergers, decreasing it by a factor of  $\simeq 20\%$ . This is simply the fact that the smaller mass stars remove less energy from the compact object binaries when interacting with them compared to the  $1 M_{\odot}$  ones, affecting in a less prominent manner the orbital evolution of these binaries (i.e. Eqs. 2 and 3). Interestingly, the choices of alternative values for  $H$  and  $K$  matter

less. The one choice of some importance to our results is changing the LMGOs mass from 3 to  $4 M_{\odot}$ . The larger mass choice increases the BH-LMGO and BH'-LMGO merger rates by  $\simeq 2$ , as the more massive LMGOs have larger exchange cross-sections in channels “A”, “C”, “J”, “L” and “R” of Fig. 1.

We have also assumed in the main text that the fraction of stars in hard binaries  $f_{\text{hard}}f_{\text{bin}}$  is 0.05. In Fig. 10, we show (at the top panel) how varying this choice affects the number of BH-LMGO, BH'-LMGO, BH-BH and BH'-BH mergers after 10 Gyrs of evolution, using the entire set of 106 Milky Way globular clusters. The low order approximation in the dynamics we consider in this work (i.e. binary-single exchanges) holds for  $f_{\text{hard}}f_{\text{bin}}$  up to about 0.05. For higher abundances of star-star binaries, the number of single compact objects quickly depletes as they form binaries with stars. Since we only include binary-single interactions there are very few compact objects that are left to participate in further binary-single exchanges. If we had included binary-binary interactions the number of cumulative mergers would only matter after 8 Gyrs of evolution. These binary-binary higher order corrections in the dynamics are insignificant in the first Gyr of the massive clusters' evolution, and become relevant only if the number of compact object-star binaries increases above the corresponding single compact object population which happens only around 9 Gyrs of evolution. For smaller clusters where the evolution is faster due to their higher central densities the binary-binary exchanges are more important but their contribution to the total merger rate is minuscule as we show in Fig. 9.

Finally, in Fig. 10 in the lower panel we show the average BH-LMGO, BH'-LMGO, BH-BH and BH'-BH mergers after 10 Gyrs, for different choices on the abundance of LMGOs in globular clusters. We define  $f_{\text{LMGO}} = 2N_{\text{LMGO}}/N_{\text{NS}}$ , where in the main text we took  $f_{\text{LMGO}} = 1$ . Changing this number is relevant if there are additional sources of LMGOs, as primordial black holes in that mass range. The number of BH-LMGO and BH'-LMGO mergers is approximately proportional to  $f_{\text{LMGO}}$  in the range shown. Instead, the numbers of merging binaries not involving a LMGO are roughly independent of  $f_{\text{LMGO}}$ .

## Appendix C: Retaining second generation black holes in clusters

In this appendix we describe how we evaluate the retention fraction of second generation black holes. In obtaining this fraction we make two assumptions. Our first assumption is that the distribution of binaries is uniform in mass ratio. The second is that the GW kick velocity follows a Maxwell-Boltzmann distribution. Our first assumption is a conservative one as binaries in a dense environments tend to exchange their members toward a mass ratio closer to unity.

The gravitational radiation from a BH binary com-

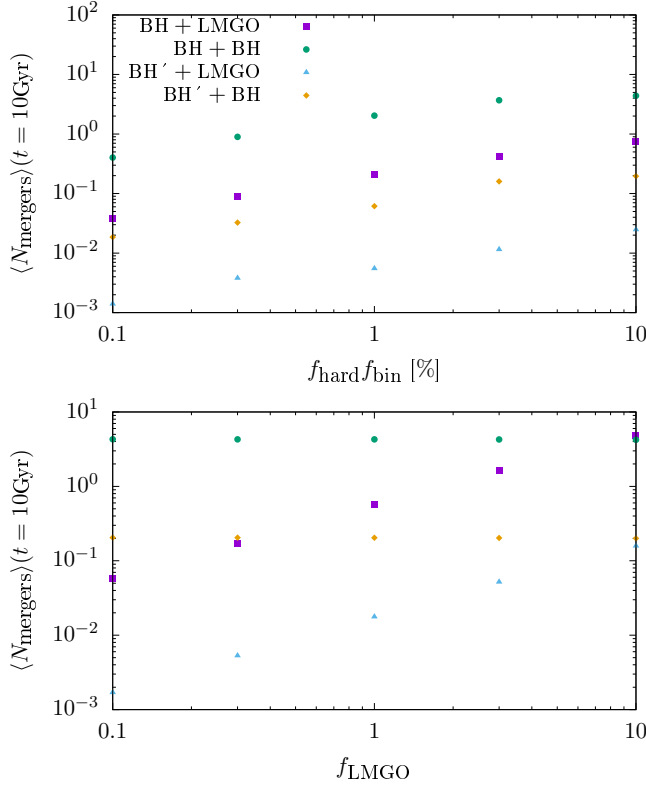


FIG. 10. The averaged number of cumulative mergers in Milky Way globular clusters, for BH-LMGO, BH'-LMGO, BH-BH and BH'-BH binaries at 10Gyr. *Top panel*, we plot the number of mergers evaluated using various choices of initial hard star-star abundances. *Bottom panel*, for the same type of merging compact object binaries we change the initial abundance of single LMGOs, parameterized as  $f_{\text{LMGO}} = 2N_{\text{LMGO}}/N_{\text{NS}}$ . In the upper panel we took  $f_{\text{LMGO}} = 1$  (our reference choice) and in the lower panel  $f_{\text{hard}}f_{\text{bin}} = 0.05$ .

posed of unequal masses is not axisymmetric. By conservation laws, the momentum carried away by the GW imparts a kick into the binary which recoils at the moment of merger where the GW radiation reaches its maximum amplitude, [80, 81]. For a binary  $m_1, m_2 \leq m_1$  and mass

ratio  $q = m_2/m_1$ , the magnitude of the GW recoil calculated for a circular orbit to 2nd post-Newtonian order and ignoring the spin of the BHs is given by [82, 83],

$$V_{\text{gw}}(q) \simeq 12 \text{Mm/s} \frac{q^2(1-q)}{(1+q)^5} \left[ 1 - 0.93 \frac{q}{(1+q)^2} \right]. \quad (\text{C1})$$

This function in Eq. (C1) obtains its maximum value 175km/s when the mass ratio is 0.362. As the kick velocity follows a Maxwell-Boltzmann distribution with parameter  $V_{\text{gw}}(q)/\sqrt{3}$ , the fraction of binary black holes retained in a cluster is,

$$f_{\text{gw}}(V_{\text{esc}}, q) = \text{erf} \left( \sqrt{\frac{3}{2}} \frac{V_{\text{esc}}}{V_{\text{gw}}(q)} \right) - \sqrt{\frac{6}{\pi}} \frac{V_{\text{esc}}}{V_{\text{gw}}(q)} \exp \left[ -\frac{3}{2} \left( \frac{V_{\text{esc}}}{V_{\text{gw}}(q)} \right)^2 \right]. \quad (\text{C2})$$

In order to estimate the fraction of second generation BH' that remain in the cluster we assume that the mass ratio of BH-BH pairs is uniformly distributed between  $q_{\text{min}}$  and 1. Taking a BH mass function, [84, 85]

$$P(m) \simeq 16 \times m^{-2.35} e^{-m/(40M_{\odot})} \Theta(m - 5M_{\odot}), \quad (\text{C3})$$

we estimate this lower value by considering three possible combinations of the form  $q_{\text{min}} = \frac{\langle m \rangle}{\langle m \rangle + \Delta m}$ ,  $q_{\text{min}} = \frac{\langle m \rangle - \Delta m}{\langle m \rangle}$  and  $q_{\text{min}} = \frac{\langle m \rangle - \Delta m}{\langle m \rangle + \Delta m}$ .  $\langle m \rangle \simeq 10M_{\odot}$  is the first moment of the distribution in Eq. (C3) and  $\Delta m \simeq 4.5M_{\odot}$ , giving us  $q_{\text{min}} = \int_{\langle m \rangle - \Delta m}^{\langle m \rangle + \Delta m} dm P(m) \simeq 0.7$ . The uniform character and hard cutoff at  $q_{\text{min}}$  is a choice that results in small numbers of retained BH's. As the majority of pairs are composed of nearly equal mass members, the mass ratio will be tilted towards unity. A more realistic mass-ratio distribution would yield higher retention fractions.

Integrating Eq. (C3) over  $q$  gives us the total retention fraction,  $F_{\text{gw}}(V_{\text{esc}})$ , of second generation BH's. Our result is depicted in Eq. 15 of the main text.

- 
- [1] William E. Harris, “A New Catalog of Globular Clusters in the Milky Way,” arXiv e-prints, arXiv:1012.3224 (2010), arXiv:1012.3224 [astro-ph.GA].
  - [2] William E. Harris, “A Catalog of Parameters for Globular Clusters in the Milky Way,” *Astron. J.* **112**, 1487 (1996).
  - [3] Alberto Sesana, Francesco Haardt, and Piero Madau, “Interaction of massive black hole binaries with their stellar environment. 1. Ejection of hypervelocity stars,” *Astrophys. J.* **651**, 392–400 (2006), arXiv:astro-ph/0604299.
  - [4] Alberto Sesana and Fazeel Mahmood Khan, “Scattering experiments meet N-body – I. A practical recipe for the

- evolution of massive black hole binaries in stellar environments,” *Mon. Not. Roy. Astron. Soc.* **454**, L66–L70 (2015), arXiv:1505.02062 [astro-ph.GA].
- [5] Carl L. Rodriguez, Sourav Chatterjee, and Frederic A. Rasio, “Binary Black Hole Mergers from Globular Clusters: Masses, Merger Rates, and the Impact of Stellar Evolution,” *Phys. Rev. D* **93**, 084029 (2016), arXiv:1602.02444 [astro-ph.HE].
- [6] Anuradha Gupta, Davide Gerosa, K.G. Arun, Emanuele Berti, Will M. Farr, and B.S. Sathyaprakash, “Black holes in the low mass gap: Implications for gravitational wave observations,” *Phys. Rev. D* **101**, 103036 (2020), arXiv:1909.05804 [gr-qc].



- [7] Giacomo Fragione and Sambaran Banerjee, “Demographics of neutron stars in young massive and open clusters,” (2020), arXiv:2006.06702 [astro-ph.GA].
- [8] Giacomo Fragione and Joseph Silk, “Repeated mergers and ejection of black holes within nuclear star clusters,” (2020), arXiv:2006.01867 [astro-ph.GA].
- [9] Johan Samsing and Kenta Hotokezaka, “Populating the Black Hole Mass Gaps In Stellar Clusters: General Relations and Upper Limits,” (2020), arXiv:2006.09744 [astro-ph.HE].
- [10] Konstantinos Kritos and Ilias Cholis, “Evaluating the merger rate of binary black holes from direct captures and third-body soft interactions using the Milky Way globular clusters,” *Phys. Rev. D* **102**, 083016 (2020), arXiv:2007.02968 [astro-ph.GA].
- [11] M. Coleman Miller and Douglas P. Hamilton, “Production of intermediate-mass black holes in globular clusters,” *Mon. Not. Roy. Astron. Soc.* **330**, 232 (2002), arXiv:astro-ph/0106188.
- [12] Simon F. Portegies Zwart and Steve L. W. McMillan, “The Runaway growth of intermediate-mass black holes in dense star clusters,” *Astrophys. J.* **576**, 899–907 (2002), arXiv:astro-ph/0201055.
- [13] M. Atakan Gurkan, Marc Freitag, and Frederic A. Rasio, “Formation of massive black holes in dense star clusters. I. mass segregation and core collapse,” *Astrophys. J.* **604**, 632–652 (2004), arXiv:astro-ph/0308449.
- [14] Ryan M. O’Leary, Frederic A. Rasio, John M. Fregeau, Natalia Ivanova, and Richard W. O’Shaughnessy, “Binary mergers and growth of black holes in dense star clusters,” *Astrophys. J.* **637**, 937–951 (2006), arXiv:astro-ph/0508224.
- [15] Ely D. Kovetz, Ilias Cholis, Marc Kamionkowski, and Joseph Silk, “Limits on Runaway Growth of Intermediate Mass Black Holes from Advanced LIGO,” *Phys. Rev. D* **97**, 123003 (2018), arXiv:1803.00568 [astro-ph.HE].
- [16] Fabio Antonini, Mark Gieles, and Alessia Gualandris, “Black hole growth through hierarchical black hole mergers in dense star clusters: implications for gravitational wave detections,” *Mon. Not. Roy. Astron. Soc.* **486**, 5008–5021 (2019), arXiv:1811.03640 [astro-ph.HE].
- [17] Jordan Flitter, Julian B. Muñoz, and Ely D. Kovetz, “Outliers in the LIGO Black Hole Mass Function from Coagulation in Dense Clusters,” (2020), arXiv:2008.10389 [astro-ph.HE].
- [18] Vishal Baibhav, Davide Gerosa, Emanuele Berti, Kaze W. K. Wong, Thomas Helfer, and Matthew Mould, “The mass gap, the spin gap, and the origin of merging binary black holes,” *Phys. Rev. D* **102**, 043002 (2020), arXiv:2004.00650 [astro-ph.HE].
- [19] K. Kritos, V. De Luca, G. Franciolini, A. Kehagias, and A. Riotto, “The Astro-Primordial Black Hole Merger Rates: a Reappraisal,” (2020), arXiv:2012.03585 [gr-qc].
- [20] Feryal Özel and Paulo Freire, “Masses, Radii, and the Equation of State of Neutron Stars,” *Ann. Rev. Astron. Astrophys.* **54**, 401–440 (2016), arXiv:1603.02698 [astro-ph.HE].
- [21] Charles D. Bailyn, Raj K. Jain, Paolo Coppi, and Jerome A. Orosz, “The Mass Distribution of Stellar Black Holes,” *Astrophys. J.* **499**, 367–374 (1998), arXiv:astro-ph/9708032 [astro-ph].
- [22] Maya Fishbach and Daniel E. Holz, “Where Are LIGO’s Big Black Holes?” *Astrophys. J. Lett.* **851**, L25 (2017), arXiv:1709.08584 [astro-ph.HE].
- [23] Daniel Wysocki, Jacob Lange, and Richard O’Shaughnessy, “Reconstructing phenomenological distributions of compact binaries via gravitational wave observations,” *Phys. Rev. D* **100**, 043012 (2019), arXiv:1805.06442 [gr-qc].
- [24] Todd A. Thompson *et al.*, “Discovery of a Candidate Black Hole - Giant Star Binary System in the Galactic Field,” (2018), 10.1126/science.aau4005, arXiv:1806.02751 [astro-ph.HE].
- [25] R. Abbott *et al.* (LIGO Scientific, Virgo), “GW190814: Gravitational Waves from the Coalescence of a 23 Solar Mass Black Hole with a 2.6 Solar Mass Compact Object,” *Astrophys. J.* **896**, L44 (2020), arXiv:2006.12611 [astro-ph.HE].
- [26] Ingo Tews, Peter T.H. Pang, Tim Dietrich, Michael W. Coughlin, Sarah Antier, Mattia Bulla, Jack Heinzl, and Lina Issa, “On the nature of GW190814 and its impact on the understanding of supranuclear matter,” (2020), arXiv:2007.06057 [astro-ph.HE].
- [27] Volodymyr Takhistov, George M. Fuller, and Alexander Kusenkov, “A Test for the Origin of Solar Mass Black Holes,” (2020), arXiv:2008.12780 [astro-ph.HE].
- [28] Nai-Bo Zhang and Bao-An Li, “GW190814’s secondary component with mass  $(2.50 - 2.67) M_{\odot}$  as a super-fast pulsar,” *Astrophys. J.* **902**, 38 (2020), arXiv:2007.02513 [astro-ph.HE].
- [29] Elias R. Most, L. Jens Papenfort, Lukas R. Weih, and Luciano Rezzolla, “A lower bound on the maximum mass if the secondary in GW190814 was once a rapidly spinning neutron star,” (2020), 10.1093/mnrasl/slaa168, arXiv:2006.14601 [astro-ph.HE].
- [30] Hung Tan, Jacquelyn Noronha-Hostler, and Nico Yunes, “Neutron Star Equation of State in light of GW190814,” (2020), arXiv:2006.16296 [astro-ph.HE].
- [31] Antonios Tsokaros, Milton Ruiz, and Stuart L. Shapiro, “GW190814: Spin and equation of state of a neutron star companion,” (2020), arXiv:2007.05526 [astro-ph.HE].
- [32] Bhaskar Biswas, Rana Nandi, Prasanta Char, Sukanta Bose, and Nikolaos Stergioulas, “GW190814: On the properties of the secondary component of the binary,” (2020), arXiv:2010.02090 [astro-ph.HE].
- [33] Yeunhwan Lim, Anirban Bhattacharya, Jeremy W. Holt, and Debdeep Pati, “Revisiting constraints on the maximum neutron star mass in light of GW190814,” (2020), arXiv:2007.06526 [nucl-th].
- [34] Daniel A. Godzieba, David Radice, and Sebastiano Bernuzzi, “On the maximum mass of neutron stars and GW190814,” (2020), arXiv:2007.10999 [astro-ph.HE].
- [35] V. Dexheimer, R.O. Gomes, T. Klähn, S. Han, and M. Salinas, “GW190814 as a massive rapidly-rotating neutron star with exotic degrees of freedom,” (2020), arXiv:2007.08493 [astro-ph.HE].
- [36] I. Bombaci, A. Drago, D. Logoteta, G. Pagliara, and I. Vidana, “Was GW190814 a black hole – strange quark star system?” (2020), arXiv:2010.01509 [nucl-th].
- [37] Zheng Cao, Lie-Wen Chen, Peng-Cheng Chu, and Ying Zhou, “GW190814: Circumstantial Evidence for Up-Down Quark Star,” (2020), arXiv:2009.00942 [astro-ph.HE].
- [38] J.W. Moffat, “Modified Gravity (MOG) and Heavy Neutron Star in Mass Gap,” (2020), arXiv:2008.04404 [gr-qc].
- [39] Artyom V. Astashenok, Salvatore Capozziello, Sergei D.



- Odintsov, and Vasilis K. Oikonomou, “Extended Gravity Description for the GW190814 Supermassive Neutron Star,” *Phys. Lett. B* **811**, 135910 (2020), arXiv:2008.10884 [gr-qc].
- [40] Sebastien Clesse and Juan Garcia-Bellido, “GW190425 and GW190814: Two candidate mergers of primordial black holes from the QCD epoch,” (2020), arXiv:2007.06481 [astro-ph.CO].
- [41] Karsten Jedamzik, “Evidence for primordial black hole dark matter from LIGO/Virgo merger rates,” (2020), arXiv:2007.03565 [astro-ph.CO].
- [42] Kyriakos Vattis, Isabelle S. Goldstein, and Savvas M. Koushiappas, “Could the  $2.6 M_{\odot}$  object in GW190814 be a primordial black hole?” (2020), arXiv:2006.15675 [astro-ph.HE].
- [43] Mohammadtaher Safarzadeh, Adrian S. Hamers, Abraham Loeb, and Edo Berger, “Formation and merging of Mass Gap Black Holes in Gravitational Wave Merger Events from Wide Hierarchical Quadruple Systems,” *Astrophys. J. Lett.* **888**, L3 (2020), arXiv:1911.04495 [astro-ph.HE].
- [44] Wenbin Lu, Paz Beniamini, and Clément Bonnerot, “On the formation of GW190814,” (2020), 10.1093/mnras/staa3372, arXiv:2009.10082 [astro-ph.HE].
- [45] Manuel Arca Sedda, “Dissecting the properties of neutron star - black hole mergers originating in dense star clusters,” *Commun. Phys.* **3**, 43 (2020), arXiv:2003.02279 [astro-ph.GA].
- [46] Sara Rastello, Michela Mapelli, Ugo N. Di Carlo, Nicola Giacobbo, Filippo Santoliquido, Mario Spera, Alessandro Ballone, and Giuliano Iorio, “Dynamics of black hole–neutron star binaries in young star clusters,” *Mon. Not. Roy. Astron. Soc.* **497**, 1563–1570 (2020), arXiv:2003.02277 [astro-ph.HE].
- [47] Manuel Arca Sedda, “Dynamical formation of the GW190814 merger,” (2021), arXiv:2102.03364 [astro-ph.HE].
- [48] Michael Zevin, Mario Spera, Christopher P.L. Berry, and Vicky Kalogera, “Exploring the Lower Mass Gap and Unequal Mass Regime in Compact Binary Evolution,” (2020), arXiv:2006.14573 [astro-ph.HE].
- [49] Mohammadtaher Safarzadeh and Abraham Loeb, “Formation of mass-gap objects in highly asymmetric mergers,” (2020), arXiv:2007.00847 [astro-ph.HE].
- [50] Tom Broadhurst, Jose M. Diego, and George F. Smoot, “Interpreting LIGO/Virgo “Mass-Gap” events as lensed Neutron Star-Black Hole binaries,” (2020), arXiv:2006.13219 [astro-ph.CO].
- [51] B.P. Abbott *et al.* (LIGO Scientific, Virgo), “GW170817: Observation of Gravitational Waves from a Binary Neutron Star Inspiral,” *Phys. Rev. Lett.* **119**, 161101 (2017), arXiv:1710.05832 [gr-qc].
- [52] B.P. Abbott *et al.* (LIGO Scientific, Virgo), “GW190425: Observation of a Compact Binary Coalescence with Total Mass  $\sim 3.4 M_{\odot}$ ,” *Astrophys. J. Lett.* **892**, L3 (2020), arXiv:2001.01761 [astro-ph.HE].
- [53] Y. Yang, V. Gayathri, I. Bartos, Z. Haiman, M. Safarzadeh, and H. Tagawa, “Black Hole Formation in the Lower Mass Gap through Mergers and Accretion in AGN Disks,” *Astrophys. J. Lett.* **901**, L34 (2020), arXiv:2007.04781 [astro-ph.HE].
- [54] Gerald D. Quinlan, “The dynamical evolution of massive black hole binaries - I. hardening in a fixed stellar background,” *New Astron.* **1**, 35–56 (1996), arXiv:astro-ph/9601092 [astro-ph].
- [55] P. C. Peters, “Gravitational Radiation and the Motion of Two Point Masses,” *Physical Review* **136**, 1224–1232 (1964).
- [56] Philip G. Breen and Douglas C. Hoggie, “Dynamical evolution of black hole sub-systems in idealised star clusters,” *Mon. Not. Roy. Astron. Soc.* **432**, 2779 (2013), arXiv:1304.3401 [astro-ph.GA].
- [57] Meagan Morscher, Bharath Pattabiraman, Carl Rodriguez, Frederic A. Rasio, and Stefan Umbreit, “The Dynamical Evolution of Stellar Black Holes in Globular Clusters,” *Astrophys. J.* **800**, 9 (2015), arXiv:1409.0866 [astro-ph.GA].
- [58] Kyle Kremer, Sourav Chatterjee, Claire S. Ye, Carl L. Rodriguez, and Frederic A. Rasio, “How Initial Size Governs Core Collapse in Globular Clusters,” *Astrophys. J.* **871**, 38 (2019), arXiv:1808.02204 [astro-ph.GA].
- [59] Eduardo Vitral and Gary A. Mamon, “Does NGC 6397 contain an intermediate-mass black hole or a more diffuse inner subcluster?” *Astron. Astrophys.* **646**, A63 (2021), arXiv:2010.05532 [astro-ph.GA].
- [60] Pavel Kroupa, “The Initial mass function of stars: Evidence for uniformity in variable systems,” *Science* **295**, 82–91 (2002), arXiv:astro-ph/0201098.
- [61] Félix Mirabel, “The Formation of Stellar Black Holes,” *New Astron. Rev.* **78**, 1–15 (2017), arXiv:1609.08411 [astro-ph.HE].
- [62] Brad M. S. Hansen and E. Sterl Phinney, “The Pulsar kick velocity distribution,” *Mon. Not. Roy. Astron. Soc.* **291**, 569 (1997), arXiv:astro-ph/9708071.
- [63] Zacharias Roupas, Grigoris Panotopoulos, and Ildio Lopes, “QCD color superconductivity in compact stars: color-flavor locked quark star candidate for the gravitational-wave signal GW190814,” (2020), arXiv:2010.11020 [astro-ph.HE].
- [64] Ishfaq Ahmad Rather, Anisul Ain Usmani, and Suresh Kumar Patra, “Hadron-Quark phase transition in the context of GW190814,” (2020), arXiv:2011.14077 [nucl-th].
- [65] Kilar Zhang and Feng-Li Lin, “Constraint on hybrid stars with gravitational wave events,” *Universe* **6**, 231 (2020), arXiv:2011.05104 [astro-ph.HE].
- [66] D. C. Hoggie, “Binary evolution in stellar dynamics,” *Mon. Not. R. Astron. Soc.* **173**, 729–787 (1975).
- [67] Monica Colpi, Michela Mapelli, and Andrea Possenti, “Probing the presence of a single or binary black hole in the globular cluster ngc 6752 with pulsar dynamics,” *Astrophys. J.* **599**, 1260–1271 (2003), arXiv:astro-ph/0309017.
- [68] <http://www.netlib.org/odepack/index.html>.
- [69] D.C. Hoggie, P. Hut, and S.L.W. McMillan, “Binary single star scattering. 7. Hard binary exchange cross-sections for arbitrary mass ratios: Numerical results and semianalytic fits,” *Mon. Not. Roy. Astron. Soc.* **318**, L61 (2000), arXiv:astro-ph/9604016.
- [70] P. A. R. Ade *et al.* (Planck), “Planck 2015 results. XIII. Cosmological parameters,” *Astron. Astrophys.* **594**, A13 (2016), arXiv:1502.01589 [astro-ph.CO].
- [71] Claire S. Ye, Wen-fai Fong, Kyle Kremer, Carl L. Rodriguez, Sourav Chatterjee, Giacomo Fragione, and Frederic A. Rasio, “On the Rate of Neutron Star Binary Mergers from Globular Clusters,” *Astrophys. J. Lett.* **888**, L10 (2020), arXiv:1910.10740 [astro-ph.HE].
- [72] Simona Miller, Thomas A. Callister, and Will Farr, “The

- Low Effective Spin of Binary Black Holes and Implications for Individual Gravitational-Wave Events,” *Astrophys. J.* **895**, 128 (2020), arXiv:2001.06051 [astro-ph.HE].
- [73] Juan Garcia-Bellido, Jose Francisco Nuño Siles, and Ester Ruiz Morales, “Bayesian analysis of the spin distribution of LIGO/Virgo black holes,” *Phys. Dark Univ.* **31**, 100791 (2021), arXiv:2010.13811 [astro-ph.CO].
- [74] M. Coleman Miller and Douglas P. Hamilton, “Four-body effects in globular cluster black hole coalescence,” *Astrophys. J.* **576**, 894 (2002), arXiv:astro-ph/0202298.
- [75] Fabio Antonini, Sourav Chatterjee, Carl L. Rodriguez, Meagan Morscher, Bharath Pattabiraman, Vicky Kalogera, and Frederic A. Rasio, “Black hole mergers and blue stragglers from hierarchical triples formed in globular clusters,” *Astrophys. J.* **816**, 65 (2016), arXiv:1509.05080 [astro-ph.GA].
- [76] Emil Khalisi, Pau Amaro-Seoane, and Rainer Spurzem, “A comprehensive nbody study of mass segregation in star clusters: energy equipartition and ejection,” *Mon. Not. Roy. Astron. Soc.* **374**, 703–720 (2007), arXiv:astro-ph/0602570.
- [77] Michele Trenti and Roeland van der Marel, “No energy equipartition in globular clusters,” *Monthly Notices of the Royal Astronomical Society* **435**, 3272–3282 (2013), arXiv:1302.2152 [astro-ph.GA].
- [78] Bence Kocsis, Merse E. Gaspar, and Szabolcs Marka, “Detection rate estimates of gravity-waves emitted during parabolic encounters of stellar black holes in globular clusters,” *Astrophys. J.* **648**, 411–429 (2006), arXiv:astro-ph/0603441.
- [79] Ivan King, “The structure of star clusters. I. an empirical density law,” *Astron. J.* **67**, 471 (1962).
- [80] Scott A. Hughes, Marc Favata, and Daniel E. Holz, “How black holes get their kicks: Radiation recoil in binary black hole mergers,” in *Conference on Growing Black Holes: Accretion in a Cosmological Context* (2004) arXiv:astro-ph/0408492.
- [81] M. J. Fitchett, “The influence of gravitational wave momentum losses on the centre of mass motion of a Newtonian binary system,” *Mon. Not. R. Astron. Soc.* **203**, 1049–1062 (1983).
- [82] M. Maggiore, *Gravitational Waves, Volume 2: Astrophysics and Cosmology* (Oxford University Press, 2018) chapter 14.3.4, pg. 252.
- [83] Carlos O. Lousto and Yosef Zlochower, “Further insight into gravitational recoil,” *Phys. Rev. D* **77**, 044028 (2008), arXiv:0708.4048 [gr-qc].
- [84] Ely D. Kovetz, Ilias Cholis, Patrick C. Breysse, and Marc Kamionkowski, “Black hole mass function from gravitational wave measurements,” *Phys. Rev. D* **95**, 103010 (2017), arXiv:1611.01157 [astro-ph.CO].
- [85] B. P. Abbott *et al.* (LIGO Scientific, Virgo), “Binary Black Hole Population Properties Inferred from the First and Second Observing Runs of Advanced LIGO and Advanced Virgo,” *Astrophys. J. Lett.* **882**, L24 (2019), arXiv:1811.12940 [astro-ph.HE].